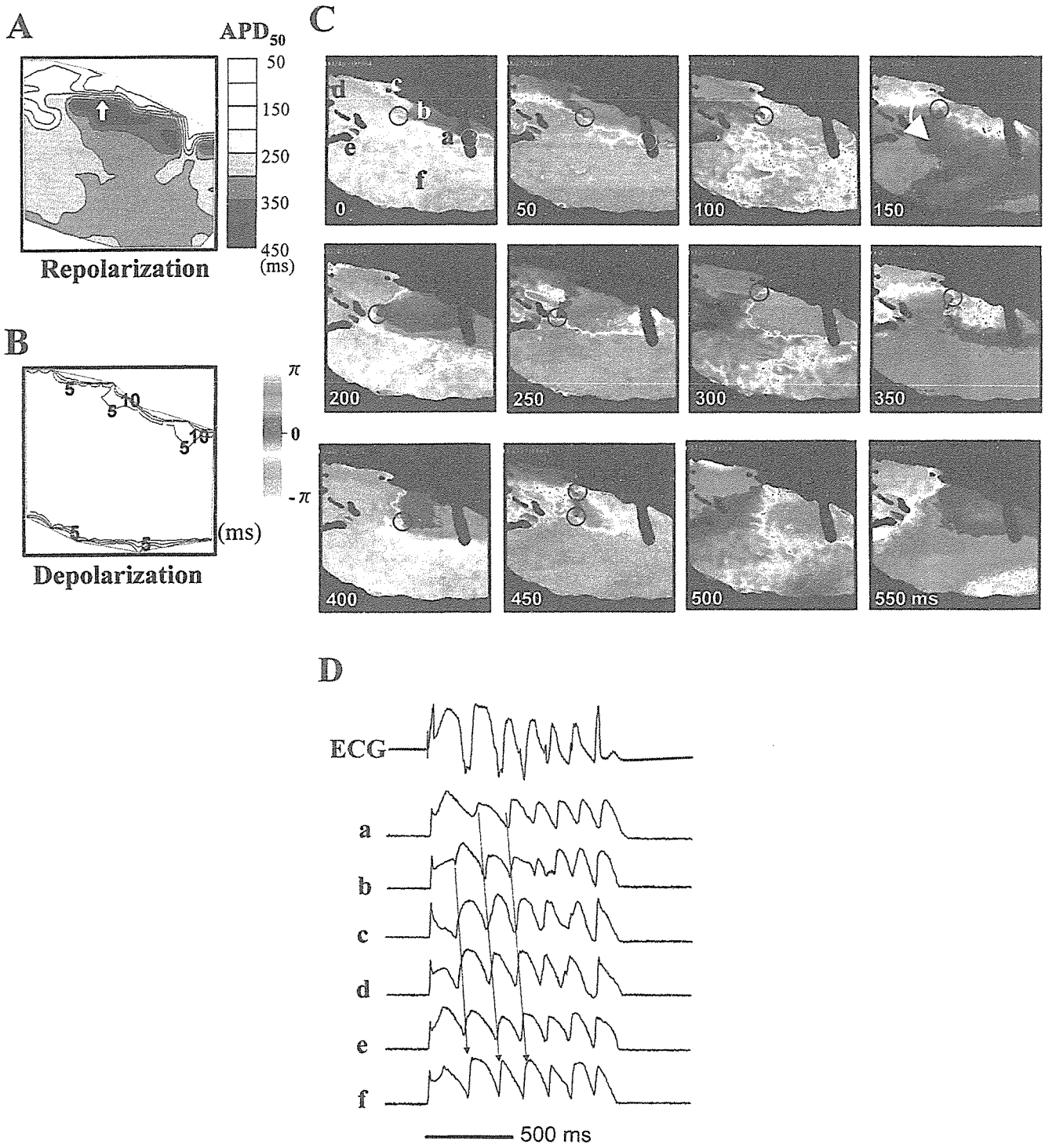

Figure 6. Representative repolarization and depolarization maps on the epicardial surface in the ST-segment elevation (Brugada-ECG) condition just before non-sustained polymorphic ventricular tachycardia (VT) (**A, B**), snapshots of phase movie during polymorphic VT originated from the epicardial phase 2 re-entry (**C**), and optical action potentials at each site (**a to f**) together with a transmural electrocardiogram (ECG) (**D**). **Open circles** = singularity points. APD_{50} = action potential duration at 50% repolarization. Please see the Appendix for accompanying video.

JACC Vol. 47, No. 10, 2006
May 16, 2006:2074–85

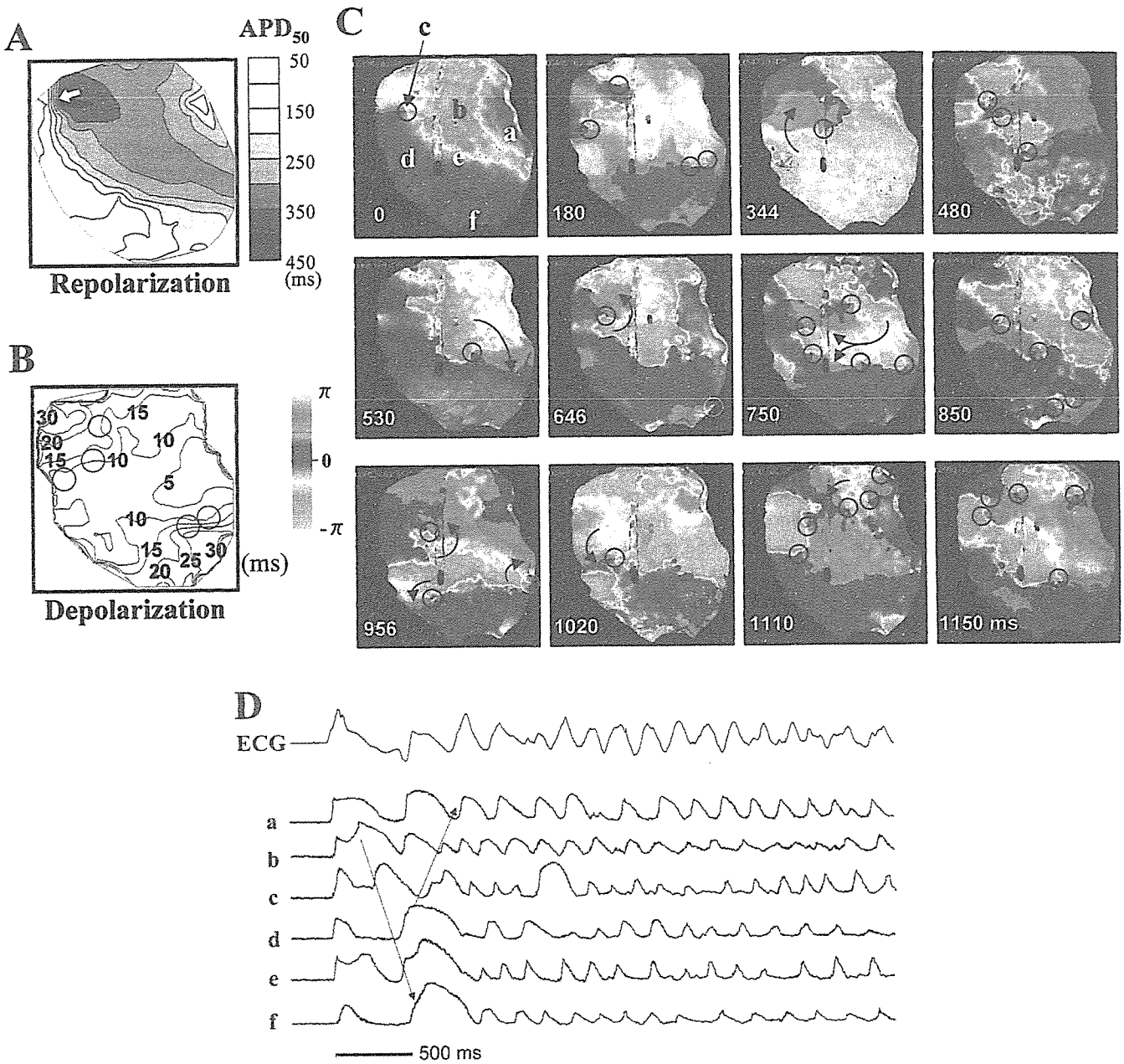

Figure 7. Representative repolarization and depolarization maps on the epicardial surface in the ST-segment elevation (Brugada-ECG) condition just before ventricular fibrillation (VF) **(A, B)**, snapshots of phase movie during VF originated from the epicardial phase 2 re-entry **(C)**, and optical action potentials at each site **(a to f)** together with a transmural electrocardiogram (ECG) **(D)**. **Open circles** = singularity points. APD_{50} = action potential duration at 50% repolarization. Please see the Appendix for accompanying videos.

supports our data that most of P2R-extrasystoles were developed from a small area (<0.5 cm) of GR_{max}.

Maintenance of VF. The only gene linked to the Brugada syndrome is cardiac sodium channel gene, *SCN5A* (17,27). Moreover, sodium channel blockades often unmask Brugada-phenotype, because a loss of sodium channels function enhances both repolarization and depolarization abnormalities (25,28,29). Our experimental study used a pure sodium channel blocker, pilsicainide, to produce the Brugada-ECG associated with prolonged QRS duration and conduction parameters; however, in the Brugada-ECG condition, the depolarization parameters were not different in beats with and without P2R-extrasystoles. In contrast, slower conduction was closely associated with VF susceptibility. These findings suggest that depolarization disturbance was not directly associated with the development of P2R-extrasystole, a trigger of VF, but might contribute to the maintenance of VF in the Brugada-ECG condition.

Electrophysiologic mechanism of VF in the Brugada syndrome has been considered to be re-entry because of high inducibility and reproducibility of VT/VF by pro-

Table 2. ECG, Optical Repolarization, and Depolarization Parameters Just Before Polymorphic VT or VF in the Brugada-ECG Condition

	PVT (n = 12)	VF (n = 5)	p Value
VT/VF CL (ms)	325 ± 33	190 ± 23	<0.001
QRS duration (ms)	74 ± 18	102 ± 23	0.009
J-point (mV)	0.48 ± 0.31	0.43 ± 0.15	NS
Epi max-min APD_{50} (ms)	394 ± 79	344 ± 88	NS
Epi GR_{max} (ms/mm)	169 ± 55	157 ± 22	NS
Sti-Epi interval (ms)	43 ± 10	60 ± 16	0.03
Delta-Epi interval (ms)	13 ± 3	41 ± 16	0.001

Values are mean ± SD.
CL = averaged tachycardia cycle length; PVT = polymorphic ventricular tachycardia; VF = ventricular fibrillation; VT = ventricular tachycardia; other abbreviations as in Table 1.

grammed electrophysiologic stimulation (3,6,14,30), although it is still unclear how VF re-entry is maintained in the Brugada syndrome. In this study, most of the polymorphic VT was single or figure-of-eight type re-entry with no wave-break and terminated within a few seconds (Fig. 6C). In contrast, wave-break in VF group occurred during the first re-entrant wave and took place at sites of the delayed epicardial conduction (Fig. 7B). Wu et al. (31) demonstrated that Ca^{2+} and fast Na^{+} current inhibition turned fast VF into slow VF by flattering APD restitution and increasing conduction time. In this Brugada model, however, VF was characterized as the shorter cycle length and multiple wandering wavelets (Fig. 7C) in spite of the slower conduction (Fig. 8), because APD restitution was not flat but rather an "inverse" pattern (Fig. 9), thus increasing dispersion of repolarization during tachycardia. Krishnan and Antzelevitch (25) had demonstrated the incremental arrhythmogenesis of Na^{+} channel dysfunction in the RV epicardium during tachycardia. Flecainide also rate-dependently slowed down the conduction velocity. Thus, fast Na^{+} current inhibition strongly enhances both heterogeneity of repolarization and conduction slowing during tachycardia in the Brugada-ECG model, which can easily break up the spiral re-entry, thus degenerating polymorphic VT into VF with multiple wavelets.

Clinical implication. Previous clinical study suggested that induction of VF by programmed ventricular stimulation depended on the severity of depolarization abnormalities such as a longer QRS duration or His-ventricular interval but did not predict the recurrence of cardiac events in symptomatic Brugada syndrome (14,15). Moreover, depolarization and repolarization abnormalities in this syndrome are now considered to be closely correlated (16,29,32,33), supporting our data that both repolarization and depolar-

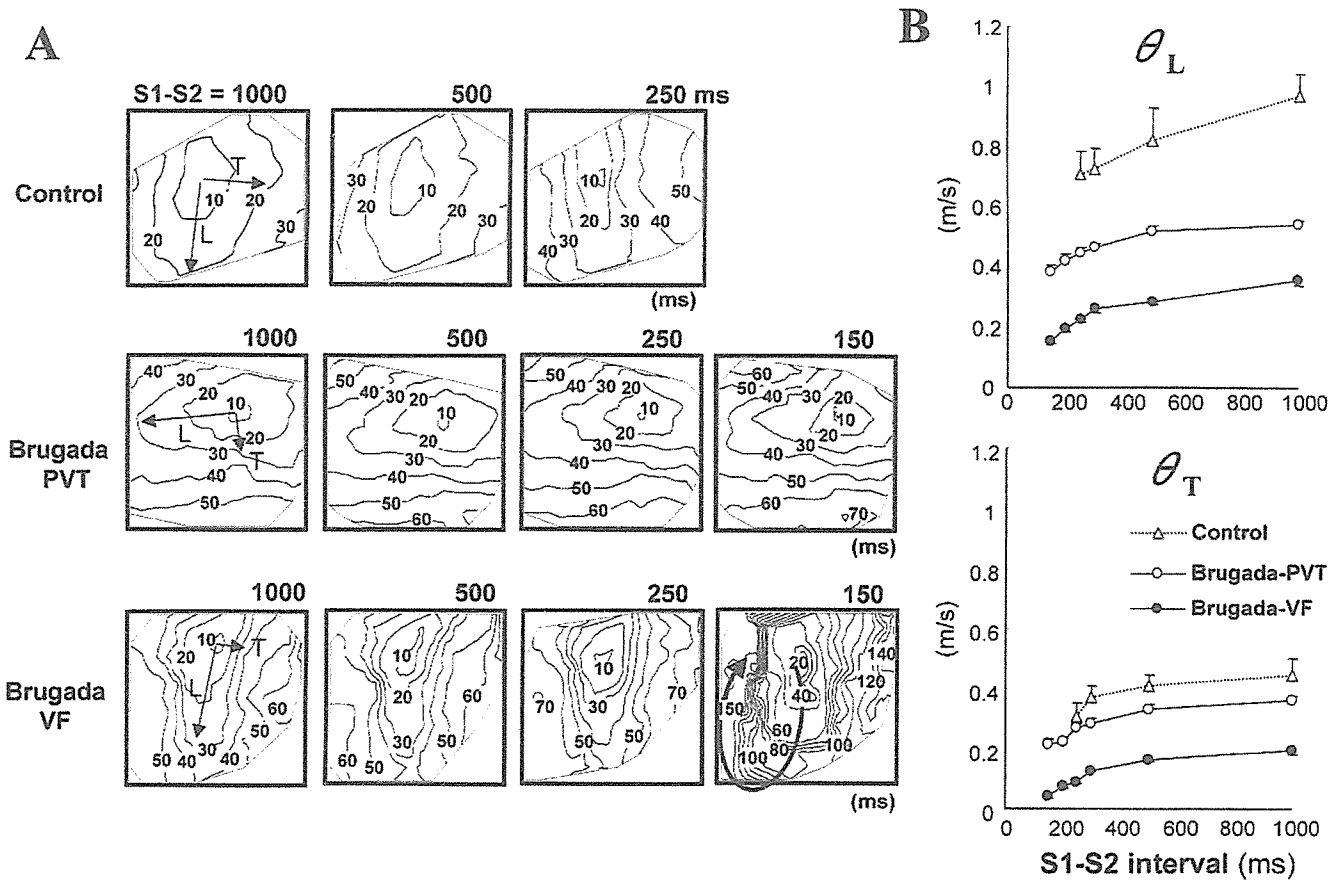

Figure 8. Representative epicardial depolarization maps paced from the epicardium by S1-S2 method in the control and ST-segment elevation (Brugada-ECG) condition with polymorphic ventricular tachycardia (PVT) or ventricular fibrillation (VF) **(A)**, and longitudinal (L) and transverse (T) conduction velocity (θ) restitution curves in each condition **(B)**. Values are mean ± SEM.

JACC Vol. 47, No. 10, 2006
May 16, 2006:2074–85

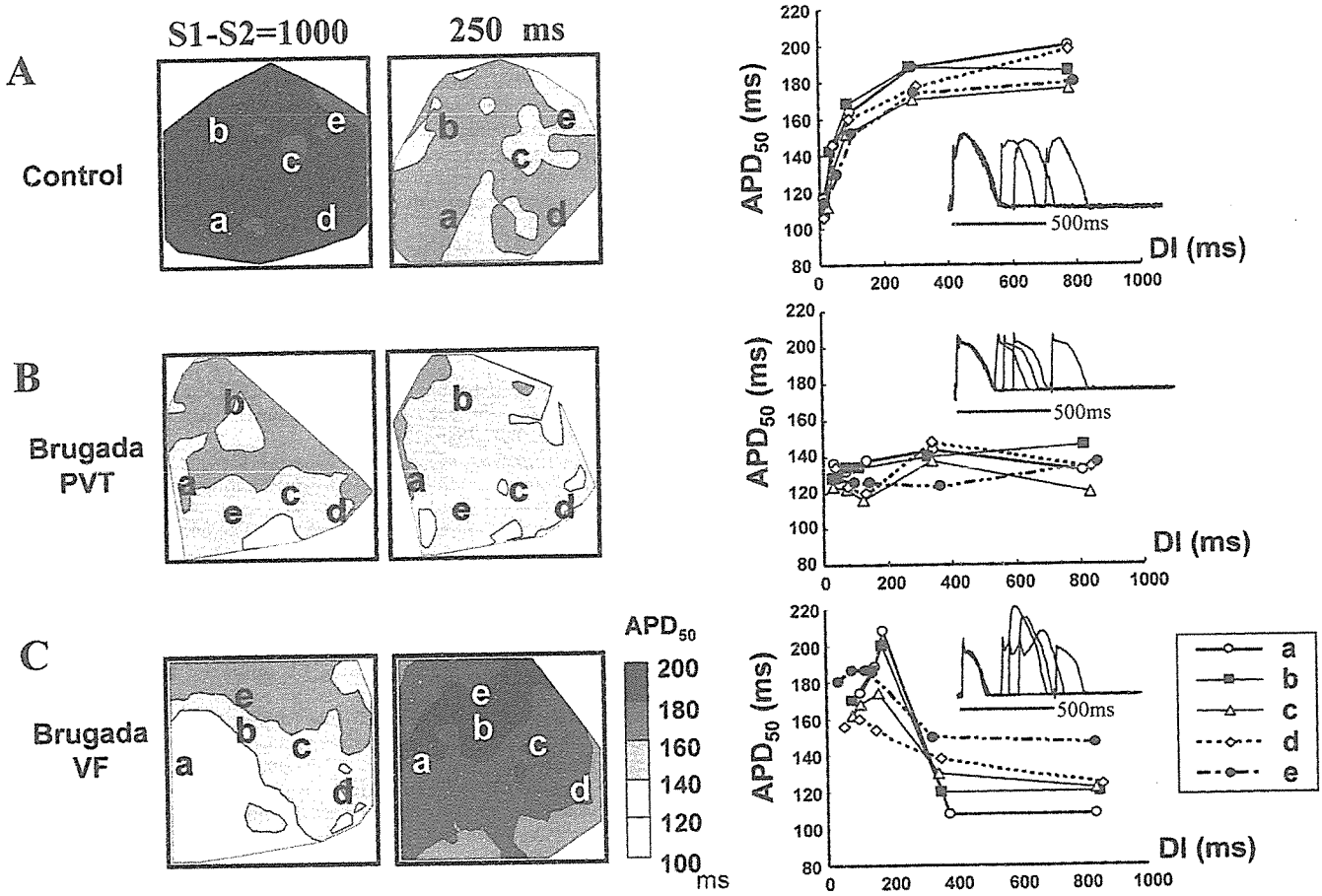

Figure 9. Representative epicardial repolarization maps paced from the epicardium by S1-S2 method and plot of the restitution of action potential duration at each site (**a to e**) and superimposed optical action potentials at site b in control condition **(A)**, and the Brugada-ECG condition with polymorphic ventricular tachycardia (PVT) **(B)** or ventricular fibrillation (VF) **(C)**. APD_{50} = action potential duration at 50% repolarization; DI = diastolic interval.

ization abnormalities were important in the development of VF. Our results, for the first time, revealed how repolarization and depolarization abnormalities interact in developing a trigger of premature ventricular complexes and in maintaining VF in the Brugada-ECG condition. A steep repolarization gradient in the epicardium introduced P2R-extrasystoles and subsequent non-sustained polymorphic VT, and further increased depolarization and repolarization abnormalities maintained VF, thus increasing risk of sudden cardiac death.

Study limitations. First, we mapped the epicardial or endocardial surface separately in each condition. Therefore, the two-dimensional mapping technique used in this study provides only limited insights into the number of spiral waves and these re-entrant patterns and could not directly evaluate the relationship between the transmural gradient of repolarization and arrhythmogenesis in the Brugada-ECG condition. A second limitation is the size of wedge preparation. It is unclear whether a polymorphic VT or VF in the wedges can result in those with larger hearts. Third, we pharmacologically created, similarly to the methods of previous studies, the Brugada-phenotype, which could not be a complete surrogate for the Brugada syndrome. Finally, with optical mapping, there is a major concern about motion artifacts that can greatly distort the AP recorded, but our ratio-metric methods can reduce motion artifacts without using an uncoupler.

Reprint requests and correspondence: Dr. Wataru Shimizu, Division of Cardiology, Department of Internal Medicine, National Cardiovascular Center, 5-7-1 Fujishiro-dai, Suita, Osaka, 565-8565 Japan. E-mail: wshimizu@hsp.ncvc.go.jp.

REFERENCES

1. Brugada P, Brugada J. Right bundle branch block, persistent ST-segment elevation and sudden cardiac death: a distinct clinical and electrocardiographic syndrome. A multicenter report. J Am Coll Cardiol 1992;20:1391–6.
2. Wilde AA, Antzelevitch C, Borggrefe M, et al. Proposed diagnostic criteria for the Brugada syndrome: consensus report. Circulation 2002; 106:2514–9.
3. Brugada J, Brugada R, Antzelevitch C, Towbin J, Nademanee K, Brugada P. Long-term follow-up of individuals with the electrocardiographic pattern of right bundle-branch block and ST-segment elevation in precordial leads V1 to V3. Circulation 2002;105:73–8.
4. Antzelevitch C, Brugada P, Borggrefe M, et al. Brugada syndrome: report of the second consensus conference: endorsed by the Heart Rhythm Society and the European Heart Rhythm Association. Circulation 2005;111:659–70.
5. Brugada J, Brugada R, Brugada P. Determinants of sudden cardiac death in individuals with the electrocardiographic pattern of Brugada

syndrome and no previous cardiac arrest. Circulation 2003;108: 3092–6.
6. Priori SG, Napolitano C, Gasparini M, et al. Natural history of Brugada syndrome: insights for risk stratification and management. Circulation 2002;105:1342–7.
7. Antzelevitch C, Brugada P, Brugada J, Brugada R, Towbin JA, Nademanee K. Brugada syndrome: 1992–2002: a historical perspective. J Am Coll Cardiol 2003;41:1665–71.
8. Yan GX, Antzelevitch C. Cellular basis for the Brugada syndrome and other mechanisms of arrhythmogenesis associated with ST-segment elevation. Circulation 1999;100:1660–6.
9. Di Diego JM, Cordeiro JM, Goodrow RJ, et al. Ionic and cellular basis for the predominance of the Brugada syndrome phenotype in males. Circulation 2002;106:2004–11.
10. Fish JM, Antzelevitch C. Role of sodium and calcium channel block in unmasking the Brugada syndrome. Heart Rhythm 2004;1:210–7.
11. Kurita T, Shimizu W, Inagaki M, et al. The electrophysiologic mechanism of ST-segment elevation in Brugada syndrome. J Am Coll Cardiol 2002;40:330–4.
12. Lukas A, Antzelevitch C. Phase 2 re-entry as a mechanism of initiation of circus movement re-entry in canine epicardium exposed to simulated ischemia. Cardiovasc Res 1996;32:593–603.
13. Nademanee K, Veerakul G, Nimmannit S, et al. Arrhythmogenic marker for the sudden unexplained death syndrome in Thai men. Circulation 1997;96:2595–600.
14. Kanda M, Shimizu W, Matsuo K, et al. Electrophysiologic characteristics and implications of induced ventricular fibrillation in symptomatic patients with Brugada syndrome. J Am Coll Cardiol 2002;39: 1799–805.
15. Ikeda T, Sakurada H, Sakabe K, et al. Assessment of noninvasive markers in identifying patients at risk in the Brugada syndrome: insight into risk stratification. J Am Coll Cardiol 2001;37:1628–34.
16. Nagase S, Kusano KF, Morita H, et al. Epicardial electrogram of the right ventricular outflow tract in patients with the Brugada syndrome: using the epicardial lead. J Am Coll Cardiol 2002;39:1992–5.
17. Smits JP, Eckardt L, Probst V, et al. Genotype-phenotype relationship in Brugada syndrome: electrocardiographic features differentiate SCN5A-related patients from non-SCN5A-related patients. J Am Coll Cardiol 2002;40:350–6.
18. Akar FG, Spragg DD, Tunin RS, Kass DA, Tomaselli GF. Mechanisms underlying conduction slowing and arrhythmogenesis in nonischemic dilated cardiomyopathy. Circ Res 2004;95:717–25.
19. Kimura M, Kobayashi T, Owada S, et al. Mechanism of ST elevation and ventricular arrhythmias in an experimental Brugada syndrome model. Circulation 2004;109:125–31.
20. Gray RA, Pertsov AM, Jalife J. Spatial and temporal organization during cardiac fibrillation. Nature 1998;392:75–8.
21. Liu YB, Peter A, Lamp ST, Weiss JN, Chen PS, Lin SF. Spatiotemporal correlation between phase singularities and wavebreaks during ventricular fibrillation. J Cardiovasc Electrophysiol 2003;14:1103–9.
22. Pitzalis MV, Anaclerio M, Iacoviello M, et al. QT-interval prolongation in right precordial leads: an additional electrocardiographic hallmark of Brugada syndrome. J Am Coll Cardiol 2003;42:1632–7.
23. Kakishita M, Kurita T, Matsuo K, et al. Mode of onset of ventricular fibrillation in patients with Brugada syndrome detected by implantable cardioverter defibrillator therapy. J Am Coll Cardiol 2000;36: 1646–53.
24. Morita H, Fukushima-Kusano K, Nagase S, et al. Site-specific arrhythmogenesis in patients with Brugada syndrome. J Cardiovasc Electrophysiol 2003;14:373–9.
25. Krishnan SC, Antzelevitch C. Flecainide-induced arrhythmia in canine ventricular epicardium. Phase 2 re-entry? Circulation 1993;87: 562–72.
26. Miyoshi S, Mitamura H, Fujikura K, et al. A mathematical model of phase 2 re-entry: role of L-type Ca current. Am J Physiol Heart Circ Physiol 2003;284:H1285–94.
27. Chen Q, Kirsch GE, Zhang D, et al. Genetic basis and molecular mechanism for idiopathic ventricular fibrillation. Nature 1998;392: 293–6.
28. Brugada R, Brugada J, Antzelevitch C, et al. Sodium channel blockers identify risk for sudden death in patients with ST-segment elevation and right bundle branch block but structurally normal hearts. Circulation 2000;101:510–5.
29. Shimizu W, Antzelevitch C, Suyama K, et al. Effect of sodium channel blockers on ST segment, QRS duration, and corrected QT interval in patients with Brugada syndrome. J Cardiovasc Electrophysiol 2000; 11:1320–9.
30. Gasparini M, Priori SG, Mantica M, et al. Programmed electrical stimulation in Brugada syndrome: how reproducible are the results? J Cardiovasc Electrophysiol 2002;13:880–7.
31. Wu TJ, Lin SF, Weiss JN, Ting CT, Chen PS. Two types of ventricular fibrillation in isolated rabbit hearts: importance of excitability and action potential duration restitution. Circulation 2002;106: 1859–66.
32. Hisamatsu K, Kusano KF, Morita H, et al. Relationships between depolarization abnormality and repolarization abnormality in patients with Brugada syndrome. J Cardiovasc Electrophysiol 2004;15:870–6.
33. Tukkie R, Sogaard P, Vleugels J, de Groot IK, Wilde AA, Tan HL. Delay in right ventricular activation contributes to Brugada syndrome. Circulation 2004;109:1272–7.

APPENDIX

For accompanying videos to Figures 5, 6, and 7, please see the online version of this article.

Electrical Space-Time Abnormalities of Ventricular Depolarization in Patients with Brugada Syndrome and Patients with Complete Right-Bundle Branch Blocks Studied by Magnetocardiography

AKIHIKO KANDORI,* TSUYOSHI MIYASHITA,* KUNIOMI OGATA,* WATARU SHIMIZU,† MIKI YOKOKAWA,† SHIRO KAMAKURA,† KUNIO MIYATAKE,† KEIJI TSUKADA,‡ SATSUKI YAMADA,£ SHIGEYUKI WATANABE,§ and IWAO YAMAGUCHI§

From the *Central Research Laboratory, Hitachi, Ltd., Higashi-Koigakubo, Kokubunji, Tokyo, Japan, †National Cardiovascular Center, Osaka, Japan, ‡Department of Electrical and Electronic Engineering, Okayama University, Okayama, Japan, £Mayo Clinic, Rochester, Minnesota, USA, §University of Tsukuba, Tsukuba, Ibaraki, Japan

KANDORI, A., ET AL.: **Electrical Space-Time Abnormalities of Ventricular Depolarization in Patients with Brugada Syndrome and Patients with Complete Right-Bundle Branch Blocks Studied by Magnetocardiography.** ***Background:*** *Both ventricular depolarization abnormalities (QRS complex) and repolarization ones (ST/T) are still controversial in literature. The objective of this study was to clarify the space-time variations that occur in patients carriers of Brugada syndrome using Magnetocardiography and also compare them with cases of complete right-bundle branch block (CRBBB) and individuals without any dromotropic disorder (control group).*

Methods and Results: *Magnetocardiograms (MCGs) of Brugada syndrome patients (n = 16), CRBBB patients (n = 14), and members of a control group (n = 46) at rest were recorded. The MCGs were used to produce a whole-heart electrical-activation diagram (W-HEAD), which can visualize the spatial time-variant activation in the whole heart. In the W-HEAD pattern, three activations were located in the left ventricle, and CRBBB patients had a wide peak with about 65-ms delay on the right anterior side. While the Brugada syndrome pattern has a posteromedian left-ventricle excitation, that is half the amplitude that occurs in CRBBB patients, the electrical conduction rate to the posterosuperior septum area was low.*

Conclusions: *The W-HEAD data made it possible to visualize space-time depolarization abnormalities. These findings suggest that the electrical conduction rate to the posterosuperior septum area in Brugada syndrome cases is low, and this low activation may be a feature of typical Brugada syndrome. (PACE 2006; 29:15–20)*

Brugada syndrome, right-bundle branch block, depolarization, arrhythmia, magnetocardiogram

Introduction

Brugada syndrome is a cardiac disorder associated with a high risk of sudden death.[1–7] The hallmark of the syndrome is a unique electrocardiogram (ECG) abnormality pattern indicating frequently atypical, pseudo incomplete or complete right-bundle branch blocks (IRBBB or CRBBB) associated with ST-segment elevation in the right precordial leads (V_1–V_2) or in anteroseptal wall (V_1–V_3).[8] The characteristic hallmark of Brugada syndrome is an inconstant and frequent pattern of IRBBB or atypical CRBBB (without S wave in left leads) associated to J point and ST-segment elevation in right precordial leads (V_1–V_2) or in the anteroseptal wall (V_1–V_3).

Address for reprints: Akihiko Kandori, Ph.D., Central Research Laboratory, Hitachi, Ltd., 1-280 Higashi-Koigakubo, Kokubunji, Tokyo 185–8601, Japan. Fax: +81-42-327-7783; e-mail: kandori@rd.hitachi.co.jp

Received May 11, 2005; revised December 8, 2005; accepted September 27, 2005.

To identify Brugada syndrome, the occurrence of ST-segment elevation in the V_1–V_3 leads is regarded as a positive response. On the basis of the occurrence, investigations on aggressive management, cellular basis, and localization of ST elevation have been performed.[9] Heterogeneity in repolarization across the ventricular wall (differences in action potential duration) of the right-ventricular outflow tract (RVOT) may be a cause of the occurrence of the ST-elevation and the genesis of ventricular tachycardia/ventricular fibrillation (VT/VF).[10] A magnetocardiogram (MCG) study,[11] which has the potential to obtain current distributions with high spatial resolution,[12] found that an abnormal current in the ST-segment elevation appears on the RVOT. However, many questions, such as a conduction pathway or an end conduction delay, concerning the depolarization abnormality in a QRS complex remain.

In the present study, we used a whole-heart electrical activation diagram (W-HEAD) for visualizing space-time depolarization variance. Using

the W-HEAD, we evaluated the differences in activation location and time delay quantitatively. Using MCG, we distinguish the difference (based on factual observation) in spatial electrical excitation in Brugada and CRBBB patients.

Methods

Subjects

We studied 16 Brugada syndrome patients (men/women: 15/1, age: 44 ± 18 years), 14 CRBBB patients (men/women: 9/5, age: 60 ± 15 years), and 46 normal control subjects (men/women: 31/15, age: 32 ± 7 years). The normal group had normal ECGs as well as a clinical history of normal physical examinations. These subjects were measured at two hospitals with capital letter (National Cardiovascular Center and Tsukuba University Hospital). The diagnosis of Brugada syndrome was based on typical ECG patterns (persistent or transient right-precordial ST-segment elevation on right precordial leads or anteroseptal wall with or without an atypical right-bundle branch block) and clinical arrhythmic events (syncope, VF, and cardiac arrest). Furthermore, according to the first Consensus about the Brugada syndrome conducted in Europe,[13] the Brugada syndrome patients were classified into the type I group (9 patients: 56%) and type II group (7 patients: 44%). In this study, we did not try to make comparisons with IRBBB, because our aim was to clarify the activation difference between CRBBB and Brugada syndrome to avoid any confusion due to the electrical time sequences of IRBBB and Brugada syndrome.

Magnetocardiogram Recordings

An MCG signal for each subject in a rest state was recorded from front and back planes above the chest over a period of 30 minutes. These signals were measured by a new magnetocardiography system (MC-6400, Hitachi, Ltd., Tokyo, Japan)[12] in a magnetically shielded room. The MCG signals were passed through an analog bandpass filter (0.1–100 Hz) and an analog notch filter (50 Hz), and then digitized at a sampling rate of 1 kHz by an analog-digital converter mounted in a PC.

Whole-Heart Electrical-Activation Diagram (W-HEAD) and Analysis

The new MCG system can make a current-arrow map (CAM)—which depicts the spatial distribution of electrical activity in the heart—with high time resolution of the front and back planes. The distribution maps in the front and back planes at each time T are used to reconstruct a W-HEAD. First, two CAMs of the front and back planes at time $T = T_0$ are joined at an angle of 0° (Fig. 1A).

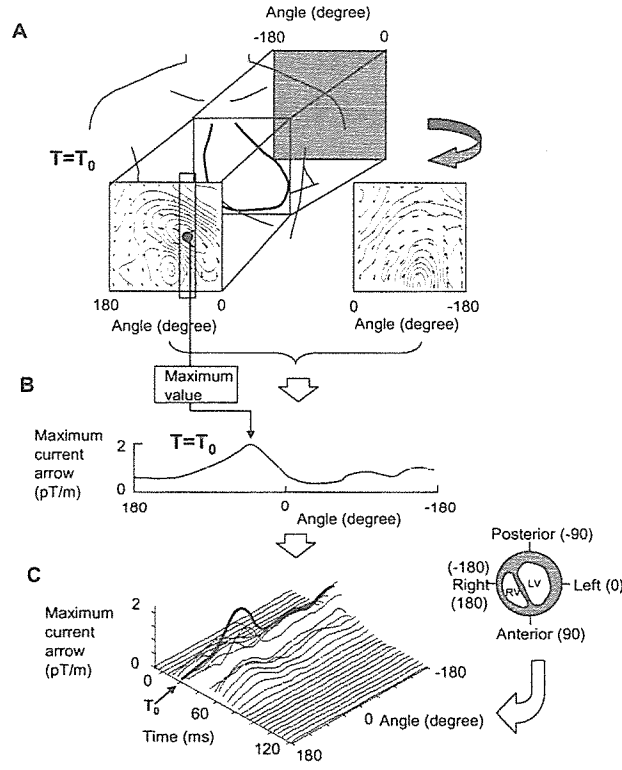

Figure 1. *Calculation method for W-HEAD. (A) Two CAMs at time $T = T_0$ produced from front and back MCG data are combined to create the W-HEAD. The angles are defined such that the right side of the heart is −180° or 180° and the left side is 0°. (B) The maximum amplitude of current arrows at time $T = T_0$ at each angle is found, and the maximum values are plotted along an axis at many angles. (C) The maximum current value at each time is drawn in the same manner. The depicted diagram can be indicated as a color map, as shown in Figure 2.*

Next, the maximum value of the current arrows along a line at each angle is found and plotted as a curve (shown in Fig. 1B). Finally, the curve at each time during the QRS complex is drawn as shown in Figure 1C. The drawings (i.e., W-HEAD), which can be redrawn as a color map (see Fig. 2), indicate the space-time changes of electrical activation.

We detected a peak value on the anterior side and one on the posterior side of the W-HEAD, and the values were plotted in terms of two parameters, angle and time. To evaluate the abnormality of delay and activated space position, the differential angle and the differential time were also computed. Furthermore, to investigate the activation magnitude of the right and left ventricles, the ratio of posterior peak to anterior peak was calculated.

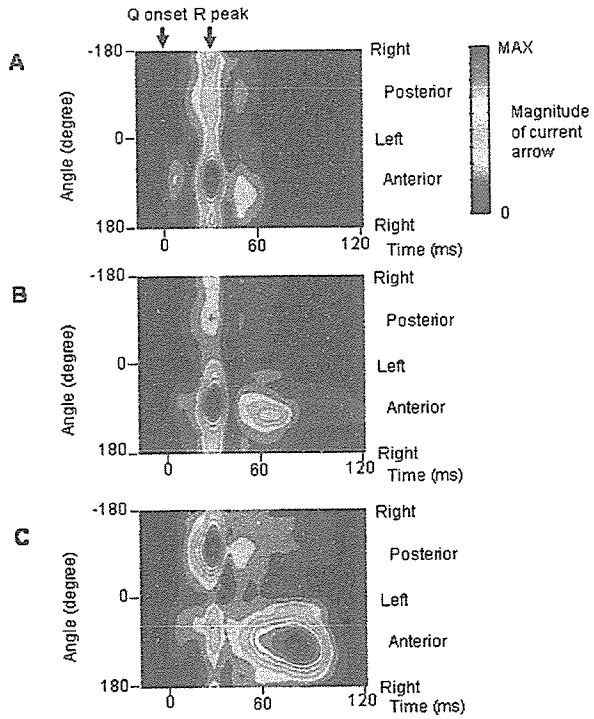

Figure 2. *W-HEAD color maps. (A) Typical control case has one peak of about 70° on the anterior side. The posterior-side peak is at an angle of −140° to −170°. The time difference between the two peaks is almost zero. (B) Typical Brugada syndrome case has a similar pattern in the case of the control anterior side, and the posterior-side peak is at −70°. At around 70 ms, some cases have a low peak as shown in this figure. (C) Typical CRBBB case has a wide pattern on the anterior side, and a sharp peak with the same anterior amplitude appears on the posterior side. The time difference between the peaks is about 75 ms.*

Results

Features of Space-Time Activation Patterns of the Control, Brugada Syndrome, and CRBBB Groups

In the control cases (Fig. 2A), a large peak appears in the anterior side (from 0° to 180°) and a lower peak in the posterior side (from 0° to −180°) due to an R-wave peak. The activation times of these peaks are close. In Figure 2A, the angle in the case of the anterior side is about 80°, that is, almost the center of the front side of the heart. On the other hand, although the posterior peak in Figure 2A is at about −160°, there were some cases near 80°. On the anterior side, two low peaks, indicating Q and S waves, respectively, occur earlier and later than the R-wave peak.

The W-HEAD pattern of Brugada syndrome patient (Fig. 2B) has a similar feature to those of the control cases. We can see two large peaks on the anterior side and one lower peak on the posterior side. The first anterior peak and the posterior peak, which are both due to the R-wave peak, appear at the same time, and the posterior peak appears at about −80°. A second anterior peak appears about 60 ms after the Q onset; this peak indicates S-wave activation.

In the W-HEAD pattern of the CRBBB patient (Fig. 2C), there are two large peaks: one with a wide spread pattern appears in the anterior area; the second has a sharp peak and appears in the posterior area. The wide peak indicates an S-wave activation in a wide QRS complex. On the other hand, although the angle of the second peak is similar to that of the peak of the Brugada syndrome patient, the strength of the second peak is higher than that of the peaks of the Brugada syndrome patient and the control. These phenomena are understandable because the electrical effects of CRBBB are limited to the terminal 60 to 80 ms of the QRS interval.

Quantitative Analysis of Space-Time Activation in the Control, Brugada Syndrome, and CRBBB Groups

The relationships between time and angle of the peaks on the anterior and posterior sides are plotted for the three main angle groups in Figure 3A. The average angle of each group—70°, −75°, and −155°—is used to discuss the electrical conduction model in Figure 5. Although the control subjects have a uniform distribution across the three groups, the data for the Brugada syndrome patients are almost completely distributed in the −75° and 70° groups. On the other hand, the data for the CRBBB patients are widely distributed in time. To understand the difference between the patient groups, we plotted the difference between the angles, i.e., Δangle (and times, i.e., Δtime) of the anterior peak and that of the posterior peak of each subject, as shown in Figure 3B. There are three clusters, defined as I, II, and III, in the plots in Figure 3B. Half the controls are in cluster I (220°–240°; <20 ms); the other half are in cluster II (120°–180°; <20 ms). The cluster-I control group has a small deviation, and average Δangle is about 228° ± 9°, while average Δtime is −1 ± 3 ms. The cluster-II control group has an average Δangle of about 155° ± 14° and an average Δtime of 0 ± 8 ms. On the other hand, 75% of Brugada syndrome patients are in cluster II. They have an average Δangle of about 160° ± 17° and an average Δtime of −2 ± 11 ms. The CRBBB patients' data (except for one) are in clusters II and III. The CRBBB patients' data in cluster II have an average Δangle of about 161° ± 16° and an average Δtime of 2 ± 9 ms, while the CRBBB patients' data in cluster III have an average Δangle of about 182° ± 33° and an average Δtime of 65 ± 8 ms.

Table I lists the number of patients from each group in each cluster. The table shows that

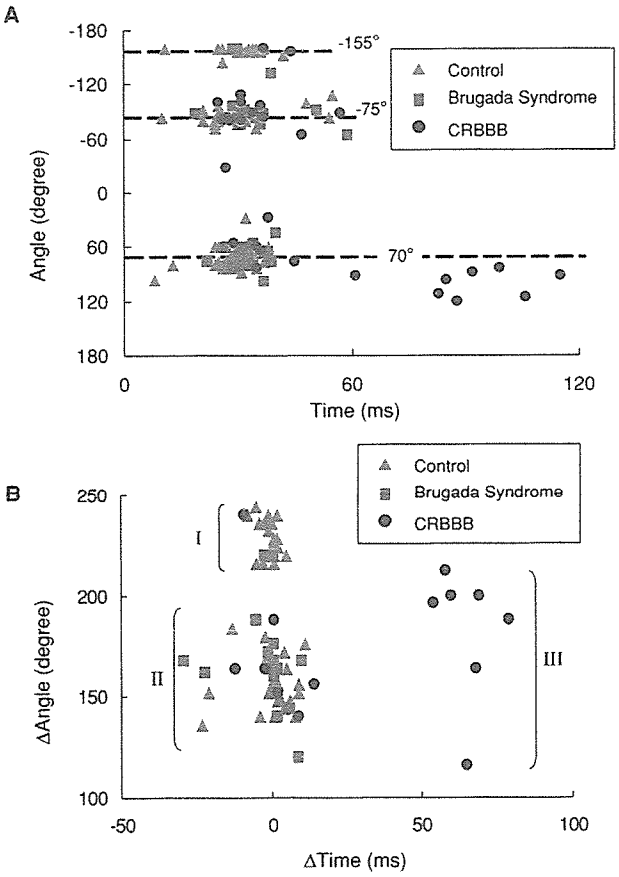

Figure 3. *Relationship between time and angle in a W-HEAD. (A) Time and angle of each peak is plotted in the figure. Three angle groups can be seen. The three angles (70°, −75°, and −155°) are used to estimate the conduction pathway in Figure 5. (B) Differences between anterior and posterior values in time and angle are calculated and the differences are plotted. The differences are classified as three clusters (I, II, and III). Cluster I is above 200° and below 30 ms. Cluster II is below 200° and below 30 ms. Cluster III is above 30 ms.*

classified cluster-III patients are all CRBBB ones. Four of the W-HEAD patterns for the CRBBB patients classified in cluster II are similar to the typical W-HEAD pattern in Figure 2C. If these four data are added to the number of patients in cluster III, 79% of CRBBB patients can be classified as being in cluster III.

The calculated ratio of the amplitudes of the anterior and posterior peaks is shown in Figure 4. The control and Brugada syndrome patients have a value around 0.5, and the CRBBB patients have a value around 1. The ratio for the CRBBB patients is significantly different ($P < 0.001$) from that for the control and Brugada syndrome patients.

Table I.

Summary of Each Cluster in Figure 3B

Group	I	II	III
Control (n = 46)	52% (24)	48% (22)	0% (0)
Brugada (n = 16)	25% (4)	75% (12)	0% (0)
CRBBB (n = 14)	7% (1)	43% (6)	50% (7)

There are three clusters in all patients. The control and Brugada syndrome patients are only in I and II. The number of Brugada syndrome patients in cluster II is higher than the other groups. Although the number of CRBBB patients is half in II and half in III, the W-HEAD pattern of four patients in cluster II is very similar to that in cluster III. If these four patients' data are counted in cluster III, the ratio for CRBBB patients goes up to 79%.

Discussion

Our W-HEAD data demonstrate the space-time difference in electrical abnormality of depolarization measurements of Brugada syndrome, CRBBB, and control patients. The difference can be described as shown in Figure 5. Three main activation positions (70°, −75°, and −155°) are defined according to the results in Figure 3A because the W-HEAD pattern and the distribution of the main peaks in Figure 2 have three main angles in Figure 3A. The three main positions agree with initial electrical activation sites reported by *in vivo* observation of the endocardium, transmural zone, and epicardial activation sequence.[14]

In the normal cases, the locations of (a), (b), and (c) are excited at almost the same time (<8 ms). The strongest excited location is position (a); the others, (b) and (c), have half its strength and about 50% probability. The three electrical pathways shown in red indicate that the strongest excitation is related to an initiation of Purkinje-muscle electrical activity. Locations (a), (b), and (c) indicate the anterosuperior septum, central region, and posterior inferior region, respectively, which are the earliest activation area.[14]

In the Brugada syndrome case, the electrical conduction to location (b) has a higher probability (75%) than in the control case. One possibility for this is that the lack of activation of the posterosuperior septum area (c) produces a conduction delay in the right ventricle, which was demonstrated in a previous body surface mapping.[15] The conduction delay results in a contraction delay of the right ventricular muscles,[16] and abnormal currents with different directions in the ST segment (in which a late potential appears and which is due to electrical activation delay) appear on the RVOT.[11] Because it was reported that VF is frequently induced in the free-wall region of the RVOT,[10] the depolarization delay in the right ventricular muscles may be related to the VF electrical origin.

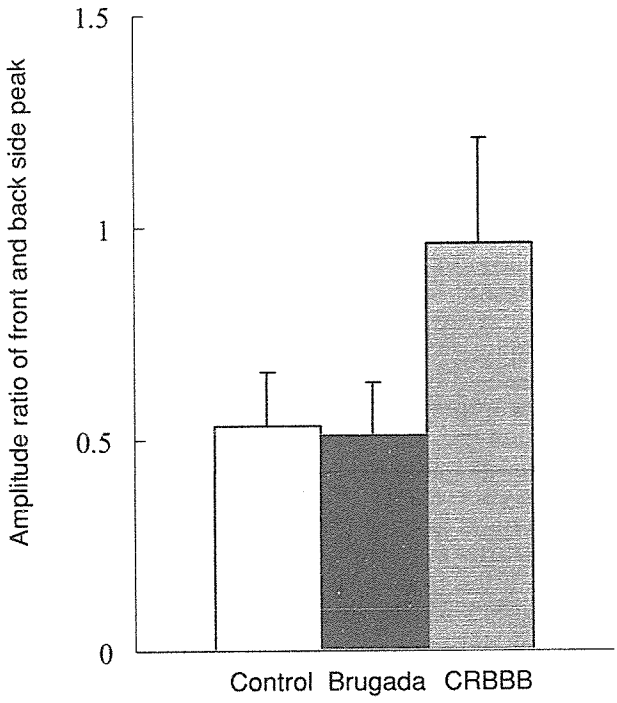

Figure 4. *Comparison of amplitude ratio between front- and back-side peaks. The ratio for CRBBB is about twice that for the control and Brugada syndrome patients. The difference has a significant P value (<0.001).*

In contrast, it can be seen in the CRBBB-patient data (Fig. 5C) that the first activation occurs at location (b), and the second activation then appears at location (a) after about 65 ms. This is understandable because electrical activation in the ventricles propagates from left to right.

In the conduction patterns of the Brugada syndrome and CRBBB patients, the predominance of posteromedian left-ventricle excitation is similar. The predominance may lead to a difficulty in identifying the ST-segment elevation. However, if a small activation in the posteromedian left ventricle is observed, the diagnosis of Brugada syndrome should be in doubt.

These observations are very similar to previous results[17] using vectorcardiogram (VCG). The results estimated by reading QRS loops in the VCG are as follows.

In most cases of Brugada syndrome, the dromotropic disorder occurs in the region of the RV free wall, after the division of the right bundle branch trunk. This is unlike most cases of CRBBB (third degree or advanced right block), where the block topographically occurs before the right branch division or in the right His, or in the membranous portion or the moderator band, before reaching the right-ventricular tip in the base

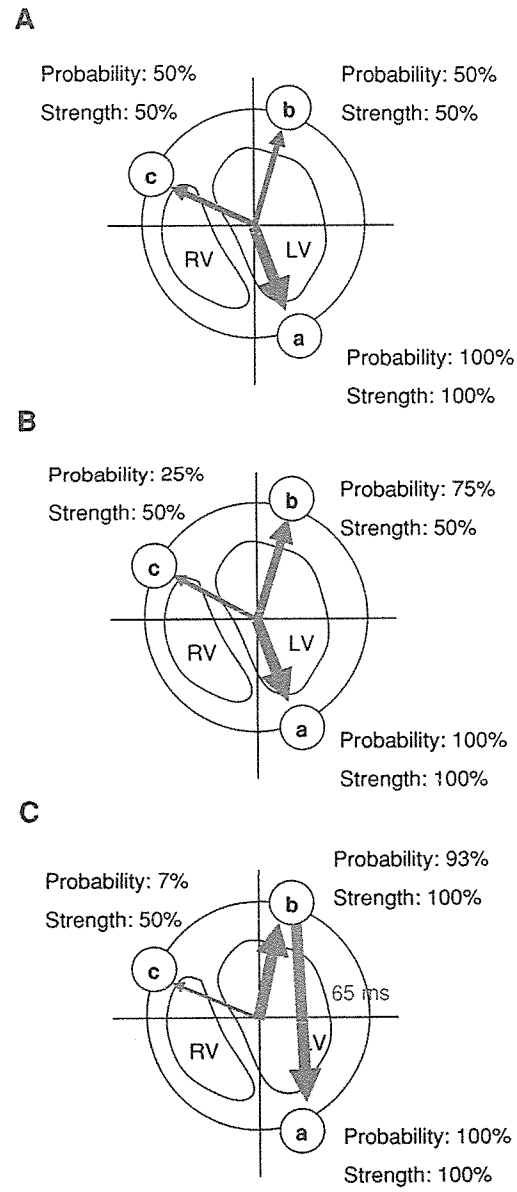

Figure 5. *Summarized conduction pathways are drawn in a spherical heart model. (A) Three pathways of the control case. The main pathway is location (a). Two pathways with 50% probability exist in posteromedian free wall (b) in left ventricle and posterosuperior septum (c). The two activation regions have 50% amplitude compared with that of anterior location (a). (B) Three pathways of the Brugada syndrome case. The probability for location (b) is higher than that of control case (A), while the strength of the activation in location (b) is similar to that of the control. The activation for location (c) is low probability, which may result in the right-ventricle activation delay and abnormality of RVOT. (C) Three pathways of the CRBBB case. The highest probability of location (b) occurs, and the location (a) is activated after location (b). The time difference is about 65 ms.*

of the papillary muscle of the tricuspid valve; i.e., the great majority of CRBBB are predivisional. The block is situated in the right His or in the main right bundle branch, while in the great majority of Brugada syndromes the block is post-divisional, right in the free wall, particularly in the superior or subpulmonary division of the right branch, located in the outflow tract of this branch.

In comparison with W-HEAD and VCG results, the depolarization is totally different between Brugada syndrome and CRBBB. The difference can be supported by the presumption that the so-called RBBB in patients with Brugada syndrome is not real RBBB.[8] The topographic differences of dromotropic disorders cause a pattern of depolarization that is completely different. In Brugada syndrome, a zonal right ventricular block with end conduction delay is eventually observed in the RVOT territory. This is called a block of the superoanterior zone of the right ventricle, located in the back and to the above right. The remainder of the right ventricle is depolarized by abnormal routes and slower than normal velocities. A right bundle branch block following a right ventriculotomy could be most likely due to this mechanism.

We showed that the ventricular depolarization of the whole heart has differences in both spatial activity and time sequence in the case of Brugada syndrome and CRBBB patients. Consequently, we conclude that the spatial and time differences shown in W-HEAD patterns can provide new knowledge that will allow us to identify and distinguish between Brugada syndrome and CRBBB patients.

Study Limitations

It is difficult to define the diagnostic criteria for Brugada syndrome by MCG due to the low prevalence of the system. We need to define the criteria based on a multicenter study. This study was also limited in several ways. First, we studied Brugada syndrome and CRBBB patients only at rest. To clarify the mechanism underlying Brugada syndrome, the variance due to sodium channel blockers induction must be investigated. Second, although the W-HEAD is a powerful tool for understanding spatial time-variant activation, our findings may differ from findings based on direct measurement of the transmembrane potential because W-HEAD is a topographic image. Furthermore, our findings may be clinically limited because so-called RBBB in patients with Brugada syndrome is not real RBBB. While our results are preliminary because of the above limitations, they are important in terms of understanding the mechanism and clinical implications of Brugada syndrome.

Acknowledgments: We are grateful to Sonoe Ito, Syuuji Hashimoto, Norio Tanaka, and Kiichi Masuda of the National Cardiovascular Center for performing the MCG measurements.

References

1. Brugada P, Brugada J. Right bundle branch block, persistent ST-segment elevation and sudden cardiac death: A distinct clinical and electrocardiographic syndrome. A multicenter report. J Am Coll Cardiol 1992; 20:1391–1396.
2. Brugada P, Brugada R, Brugada J. Sudden death in patients and relatives with the syndrome of right bundle branch block, ST segment elevation in the precordial leads V(1) to V(3) and sudden death. Eur Heart J 2000; 21:321–326.
3. Brugada R, Brugada J, Antzelevitch C, et al. Sodium channel blockers identify risk for sudden death in patients with ST-segment elevation and right bundle branch block but structurally normal hearts. Circulation 2000; 101:510–515.
4. Ikeda T. Brugada syndrome: Current clinical aspects and risk stratification. Ann Electrocardiol 2002; 7:251–262.
5. Priori SG, Napolitano C, Gasparini M, et al. Clinical and genetic heterogeneity of right bundle branch block and ST-segment elevation syndrome: A prospective evaluation of 52 families. Circulation 2000; 102:2509–2515.
6. Shimizu W, Antzelevitch C, Suyama K, et al. Effect of sodium channel blockers on ST segment, QRS duration, and corrected QT interval in patients with Brugada syndrome. J Cardiovasc Electrophysiol 2000; 11:1320–1329.
7. Shimizu W, Matsuo K, Takagi M, et al. Body surface distribution and response to drugs of ST segment elevation in Brugada syndrome: Clinical implication of eighty-seven-lead body surface potential mapping and its application to twelve-lead electrocardiograms. J Cardiovasc Electrophysiol 2000; 11:396–404.
8. Antzelevitch C, Brugada P, Borggrefe M, Brugada J, Brugada R, Corrado D, Gussak I, LeMarec H, Nademanee K, Perez Riera AR, Shimizu W, Schulze-Bahr E, Tan H, Wilde A. Brugada syndrome: Report of the second consensus conference. Heart Rhythm 2005; 2:429–440.
9. Yan GX, Antzelevitch C. Cellular basis for the Brugada syndrome and other mechanisms of arrhythmogenesis associated with ST segment elevation. Circulation 1999; 100:1660–1666.
10. Morita H, Fukushima-Kusano K, Nagase S, et al. Site-specific arrhythmogenesis in patients with Brugada syndrome. J Cardiovasc Electrophysiol 2003; 14:373–379.
11. Kandori A, Shimizu W, Yokokawa M, et al. Identifying patterns of spatial current dispersion that characterize and separate the Brugada syndrome and complete right-bundle branch block. Med Biol Eng Comput 2004; 42:236–244.
12. Kandori A, Shimizu W, Yokokawa M, et al. Detection of spatial repolarization abnormalities in patients with LQT1 and LQT2 forms of congenital long-QT syndrome. Physiol Meas 2002; 23:603–614.
13. Wilde AA, Antzelevitch C, Borggrefe M, Brugada J, Brugada R, Brugada P, Corrado D, Hauer RN, Kass RS, Nademanee K, Priori SG, Towbin JA. Study group on the molecular basis of arrhythmias of the European Society of Cardiology. Eur Heart J 2002; 23:1648–1654.
14. Durrer D, van Dam RT, Freud GE, et al. Total excitation of the isolated human heart. Circulation 1970; 41:899–912.
15. Kasanuki H, Ohnishi S, Ohtsuka M, et al. Idiopathic ventricular fibrillation induced with vagal activity in patients without obvious heart disease. Circulation 1997; 95:2277–2285.
16. Tukkie R, Sogard P, Vleugels J, et al. Delay in right ventricular activation contributes to Brugada syndrome. Circulation 2004; 109:1272–1277.
17. Pérez Riera AR, Ferreira C, Schapachnik E. Value of 12 lead electrocardiogram and derived methodologies in the diagnosis of Brugada disease (Ch. 7). In: Antzelevitch C (ed.) with associate editors Brugada P, Brugada J, Brugada R. The Brugada Syndrome: From Bench to Bedside. Oxford, Blackwell-Futura, 2004, pp. 87–110.

Spatial Distribution of Repolarization and Depolarization Abnormalities Evaluated by Body Surface Potential Mapping in Patients with Brugada Syndrome

MIKI YOKOKAWA, M.D.,* HIROSHI TAKAKI, M.D.,† TAKASHI NODA, M.D., PH.D.,* KAZUHIRO SATOMI, M.D., PH.D.,* KAZUHIRO SUYAMA, M.D., PH.D.,* TAKASHI KURITA, M.D., PH.D.,* SHIRO KAMAKURA, M.D., PH.D.,* and WATARU SHIMIZU M.D., PH.D.*

From the *Division of Cardiology, Department of Internal Medicine, and †Department of Cardiovascular Dynamics, National Cardiovascular Center, Suita, Japan

Background: *Mutations in sodium channel gene, SCN5A, have been identified in Brugada syndrome, but it is still unclear as to how sodium channel dysfunction relates to arrhythmogenesis. We examined spatial distribution of both repolarization and depolarization abnormalities in patients with Brugada syndrome by using 87-leads body surface potential mapping (BSPM).*

Methods: *BSPM was recorded under baseline condition and after pharmacological interventions in 28 patients with Brugada syndrome (27 males, 49 ± 14 years). The ST-segment amplitude 20 ms after the end of QRS (ST20), QRS duration, and corrected recovery time (RTc) were measured in all 87-leads, and averaged among 6-leads (D–F, 5–6) reflecting right ventricular outflow tract (RVOT) potentials and the other 81-leads.*

Results: *The ST20 was elevated at baseline, normalized by isoproterenol, and augmented by pilsicainide in only the RVOT. The RTc was longer at baseline and increased by pilsicainide in only the RVOT. On the other hand, the QRS duration was slightly widened at baseline, further increased by pilsicainide, but not changed by isoproterenol in both leads.*

Conclusions: *The ST-segment elevation and the RTc prolongation were localized and modulated by agents only in the RVOT region, while the slight QRS widening at baseline and further increase by pilsicainide were observed homogeneously. Our data suggest that depolarization abnormalities are distributed homogeneously, whereas repolarization abnormalities are localized in the RVOT. (PACE 2006; 29:1112–1121)*

brugada syndrome, ST-segment, body surface potential mapping, repolarization, depolarization

Introduction

Brugada syndrome is characterized by an accentuated ST-segment elevation in the right precordial leads V1 through V3, reflecting potentials of the right ventricular outflow tract (RVOT) and generally associated with sudden cardiac death secondary to a rapid polymorphic ventricular tachycardia (PVT) or ventricular fibrillation (VF).[1–10] In Brugada syndrome, both repolarization and depolarization abnormalities have been reported.[11–14] Transmural electrical heterogeneity of repolarization across the wall of the RVOT is thought to cause ST-segment elevation in the leads V1-V3.[15,16] On the other hand, depolarization abnormalities including prolongation of the P wave, QRS duration, and PR interval are frequently observed in patients with Brugada syndrome.[12] Mutations in sodium channel gene, *SCN5A*, have been identified in Brugada syndrome, but it is still unclear as to how depolarization abnormalities by sodium channel dysfunction relate to arrhythmogenesis.[17,18]

In the present study, we examined the spatial distribution of both repolarization and depolarization abnormalities in patients with Brugada syndrome by using 87-leads body surface potential mapping (BSPM) under baseline condition and after pharmacological interventions.

Methods

Patients Population

The study population consisted of 28 patients with Brugada syndrome who were admitted to the National Cardiovascular Center, Suita, Japan, between 2000 and 2004 (27 men, aged 17–72 years; mean 49 ± 14). Brugada syndrome was diagnosed

Address for reprints: Wataru Shimizu, M.D., Ph.D., Division of Cardiology, Department of Internal Medicine, National Cardiovascular Center, 5-7-1 Fujishiro-dai, Suita, Osaka 565-8565, Japan. Fax: +81-6-6872-7486; e-mail: wshimizu@hsp.ncvc.go.jp

Received April 3, 2006; revised June 7, 2006; accepted June 21, 2006.

when a Type 1 coved-type ST-segment elevation (≥0.2 mV at J point) was observed in more than one of the right precordial leads (V1 to V3) in the presence or absence of a sodium channel blocker, and in conjunction with one of the following: (1) documented VF or PVT, (2) a family history of sudden cardiac death at age < 45 years, Type 1 electrocardiogram (ECG) in family members, (3) inducibility of VF or PVT with programmed electrical stimulation, and (4) a history of aborted cardiac arrest with or without documentation of VF, syncopal episodes of unknown origin, or nocturnal agonal respiration.

The clinical characteristics of the 28 patients are shown in Table I. Seventeen patients (61%) had Type 1 coved-type ST-segment elevation in the baseline standard 12-leads ECG, while the remaining 11 patients showed Type 1 ECG after intravenous injection of sodium channel blockers. VF was documented in 4 patients (14%), 13 patients (46%) had syncopal episodes only, and the remaining 11 patients were asymptomatic. Nine patients (32%) had a family history of sudden cardiac death. Twenty-four patients underwent programmed ventricular electrical stimulation during electrophysiological study, and VF was induced in 19 of the 24 patients (79%). A mutation in the *SCN5A* was identified in four patients (14%).

Body Surface Potential Mapping

Eighty-seven-leads BSPM was recorded using a VCM-3000 (Fukuda Denshi Co., Tokyo, Japan) (Fig. 1).[19,20] Eighty-seven-leads were arranged in a lattice-like pattern (13 × 7 matrix), except for four leads on the mid-axillary lines, which covered the entire thoracic surface; 59-leads were located on the anterior chest (Columns A–I) and 28-leads on the back (Columns J–M). These 87-unipolar electrograms with Wilson's central terminals as a reference, the standard 12-leads ECG, and Frank X, Y, Z scalar leads were recorded simultaneously. Row 6 of the BSPM was coincident with the level of the parasternal second intercostal space, whereas row 4 coincided with the mid-clavicular fifth intercostal space. Columns A and I of the BSPM were located on the right and left mid-axillary lines, whereas column E was on the mid-sternal line. Columns C and G corresponded to the right and left mid-clavicular lines. Therefore, leads V1 and V2 of the 12-leads ECG were located between D5 and E5, and between E5 and F5 of the BSPM leads. The six particular leads (D–F, 5–6) were defined as representative of the RVOT area based on the data of our previous study.[21] The ECG data were scanned with multiplexers and digitized using analog-to-digital converters with a sampling rate of 1,000 samples/second per channel. The digitized data were stored on a floppy disk and transferred to a personal computer with the analysis program developed by our institution.

Table I.

Clinical Characteristics of the 28 Patients with Brugada Syndrome

Male/Female	27/1
Age (years)	49 ± 14 (17–72)
Spontaneous Type 1 ECG	17 (61%)
Documented VF	4 (14%)
Syncopal episode of unknown origin	13 (46%)
Family history of SCD	9 (32%)
Induced VF during EPS	19/24 (79%)
Positive for *SCN5A* mutation	4 (14%)
ICD implantation	21 (75%)

Values are mean ± SD for age. Age represents the age at which diagnosis of Brugada syndrome was made.
ECG = electrocardiogram; EPS = electrophysiological study; ICD = implantable cardioverter-defibrillator; SCD = sudden cardiac death; VF = ventricular fibrillation.

Repolarization and Depolarization Parameters in ECGs

In the present study, three parameters were evaluated (Fig. 2). As the repolarization parameters, we measured the amplitude of ST-segment 20 ms after the end of QRS (ST20) and recovery time (RT) defined as the interval between QRS-onset and maximum dV/dt point of T wave. The RTc was corrected by Bazett's method ($RTc = RT/\sqrt{RR}$), as previously reported.[19] As the depolarization parameter, QRS duration was measured. Each parameter was measured semi-automatically in all 87-leads by the computer analysis program developed by our institution. We averaged these ECG parameters among 6-leads ECG (D–F, 5–6) in the upper precordial region reflecting the RVOT potentials and among the remaining 81-leads ECG reflecting potentials of other region (Fig. 1), and then compared data between the two regions.

Algorithm for Determination of the End of QRS

The end of QRS (QRS-end) is difficult to determine especially in the right precordial leads manifesting ST-segment elevation in Brugada patients. Figure 3 illustrates the algorithm for determination of the QRS-end in each BSPM ECG. With superimposed 87-leads ECG, we first determined the onset of QRS by detecting the earliest deflection, and then determined the QRS-end provisionally by visual inspection of all 87-leads (Fig. 3, upper panel). Thereafter, we computed the first derivative of QRS voltage (dV/dt) in each lead and its algebraic summation of the absolute value indicated by the area colored in black (Fig. 3, lower panel).

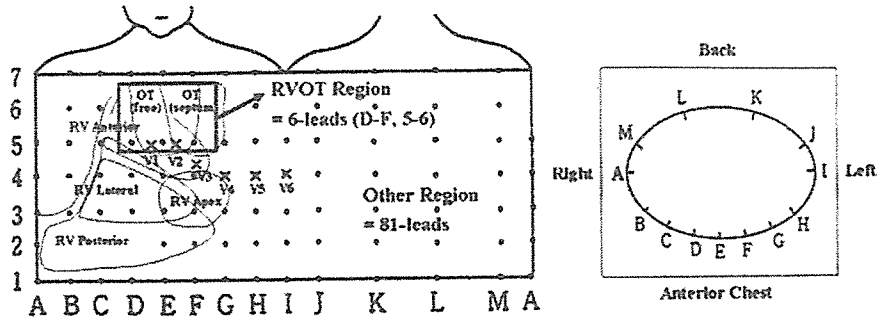

Figure 1. *Eighty-seven-leads body surface electrocardiogram (ECG). Plot of 87 unipolar electrode sites (•). Eighty-seven-leads points are arranged in a lattice-like pattern (13 × 7 matrix), except for 5 lead points on both mid-axillary lines, and covered the entire thoracic surface. The location of precordial 6 leads, V1–V6 in the 12-leads ECG is indicated by X. V1 and V2 leads of the ECG are located between D5 and E5, and between E5 and F5, respectively. The area of 6-leads ECG (D–F, 5–6) in the upper precordial area is defined as the RVOT region.*

The QRS-end was defined as the time-point where the cumulative area from the QRS-onset reached 98% of the total area.[22,23]

Pharmacological Interventions

After recording BSPM under baseline condition (Baseline-BSPM), isoproterenol, a β-adrenergic agonist, was infused at a constant rate of 0.02 $\mu gkg^{-1}min^{-1}$. When steady heart rate was achieved by isoproterenol infusion, BSPM was recorded (Isoproterenol-BSPM). After the effect of isoproterenol was completely washed out, pilsicainide, a class IC sodium channel blocker, was injected (5 mg every 1 minute) upto a maximum dose of 1 $mgkg^{-1}$ or 50 mg. BSPM was recorded 5 minutes after the completion of the drug, when the effect of the drug reached steady state (Pilsicainide-BSPM). Pilsicainide injection was stopped when Type 1 coved ST-segment elevation appeared or additional J-point elevation of $\geq$0.2 mV in case of baseline saddleback-type ST-segment was observed. Pilsicainide was also stopped when QRS duration was increased by $\geq$130% or spontaneous premature ventricular contractions were induced.

We compared the ECG parameters averaged among 6-leads of the RVOT region with those among 81-leads of the other region at baseline condition, after isoproterenol infusion, and pilsicainide injection.

Statistical Analysis

Numerical values were expressed as means ± SD, unless otherwise indicated. Comparisons of parameters before and after pharmacological interventions and those of each parameter between the 6-leads and 81-leads were made by using two-way repeated measures analysis of variance (ANOVA), followed by Scheffe's test. Comparisons of changes (Δ) in parameters with pharmacological interventions between the 6-leads and 81-leads were made

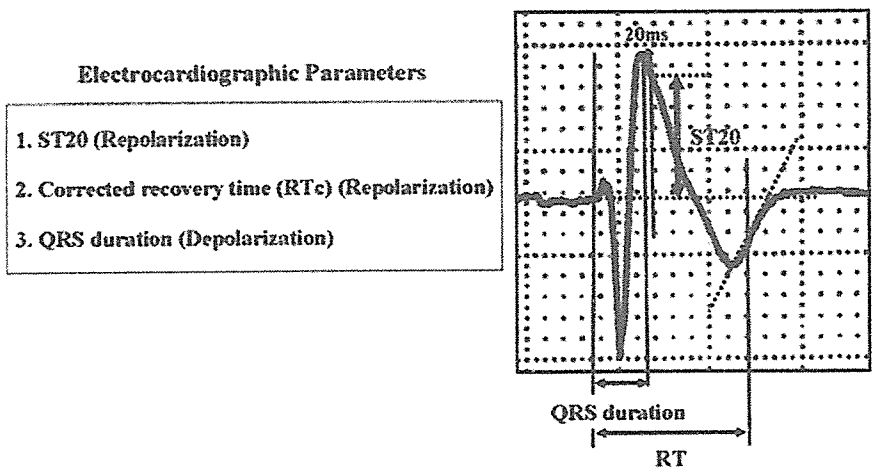

Figure 2. *Electrocardiographic parameters. As the repolarization parameters, the ST20 and corrected recovery time (RTc) were evaluated. The ST20 was defined as the amplitude of the ST-segment 20 ms after the end of QRS. The recovery time (RT) was defined as the interval between QRS-onset and maximum dV/dt point of T wave. As the depolarization parameter, the QRS duration was evaluated. Each parameter was measured semi-automatically in all 87-leads.*

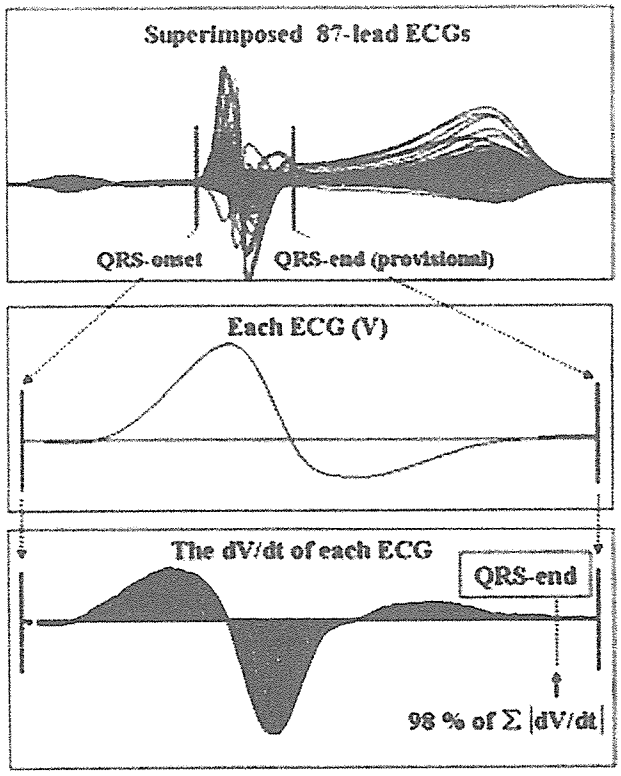

Figure 3. *The algorithm for determination of the end of QRS (QRS-end) in each electrocardiogram. With superimposed 87-leads ECG, the onset of QRS was first determined by detecting the earliest deflection, and then the QRS-end was provisionally determined by visual inspection of all 87-leads. Thereafter, the first derivative of QRS voltage (dV/dt) and its algebraic summation of the absolute value indicated by the area colored in black were computed in each lead. The QRS-end was defined as the time-point where the cumulative area from the QRS-onset reached 98% of the total area.*

by using one-way ANOVA, followed by Scheffe's test. A P value < 0.05 was considered significant.

Results

Figure 4A–C shows the 87-leads ECG (a) and 6-leads ECG, reflecting potentials of the RVOT region (b) in a representative patient with Brugada syndrome.

ECG Parameters in the RVOT Region and the Other Region Before and After Pharmacological Interventions

Figure 5A–C depicts composite data of each ECG parameter of 6-leads and 81-leads before and after pharmacological interventions in the 28 patients with Brugada syndrome.

The ST-segment was elevated under baseline condition only in 6-leads, and the baseline ST20 was significantly higher in 6-leads than in 81-leads (0.22 ± 0.10 mV vs 0.02 ± 0.02 mV; $P < 0.0005$) (Fig. 5A). In 6-leads reflecting the RVOT potentials, the ST20 was decreased by isoproterenol (0.11 ± 0.09 mV; $P < 0.0005$ vs baseline) and augmented by pilsicainide (0.33 ± 0.11 mV; $P < 0.0005$ vs baseline) significantly (Fig. 5A, left panel). In contrast, the ST20 was not changed in 81-leads after pharmacological interventions (Isoproterenol: 0.01 ± 0.01 mV; Pilsicainide: 0.01 ± 0.02 mV; P = N.S. vs baseline) (Fig. 5A, right panel).

The baseline RTc was significantly longer in 6-leads than in 81-leads (325 ± 46 ms vs 302 ± 24 ms; $P < 0.05$) (Fig. 5B). Isoproterenol infusion slightly prolonged the RTc in 81-leads (327 ± 28 ms; $P < 0.05$ vs baseline) (Fig. 5B, right panel). The RTc was further prolonged by pilsicainide only in 6-leads (354 ± 42 ms; $P < 0.005$ vs baseline) (Fig. 5B, left panel), while it was not changed by pilsicainide in 81-leads (309 ± 23 ms) (Fig. 5B, right panel).

The baseline QRS duration was slightly prolonged both in 6-leads and 81-leads, but not different between the two regions (107 ± 14 ms vs 104 ± 14 ms; P = N.S.) (Fig. 5C). In both regions, the QRS duration was not changed by isoproterenol (6-leads: 106 ± 14 ms; 81-leads: 103 ± 14 ms; P = N.S. vs baseline, respectively), but further increased by pilsicainide (6-leads: 125 ± 18 ms; 81-leads: 121 ± 18 ms; $P < 0.0005$ vs baseline, respectively). However, the prolongation of the QRS duration with pilsicainide was homogeneous between the two regions.

Comparison of Changes (Δ) of ECG Parameters with Pharmacological Intervention Between the RVOT Region and the Other Region

Figure 6A and B illustrates comparison of changes (Δ) of each ECG parameter with isoproterenol and pilsicainide between 6-leads and 81-leads in the 28 patients with Brugada syndrome.

During isoproterenol infusion, the ΔST20 was significantly larger in 6-leads than in 81-leads (-0.12 ± 0.09 mV vs -0.01 ± 0.01 mV; $P < 0.0005$). Both ΔRTc and ΔQRS duration were not different between the two regions (ΔRTc: 6-leads, 19 ± 39 ms vs 81-leads, 25 ± 24 ms; ΔQRS duration: 6-leads, -1 ± 3 ms vs 81-leads, -1 ± 3 ms; P = N.S., respectively).

After pilsicainide injection, the ΔST20 was significantly larger in 6-leads than in 81-leads (0.10 ± 0.05 mV vs 0.00 ± 0.01 mV; $P < 0.0005$). The ΔRTc was also significantly larger in 6-leads than in 81-leads (28 ± 38 ms vs 7 ± 17 ms; $P < 0.05$). In contrast, the ΔQRS duration was not different between the two regions (6-leads: 18 ± 12 ms vs 81-leads: 17 ± 9 ms; P = N.S.).

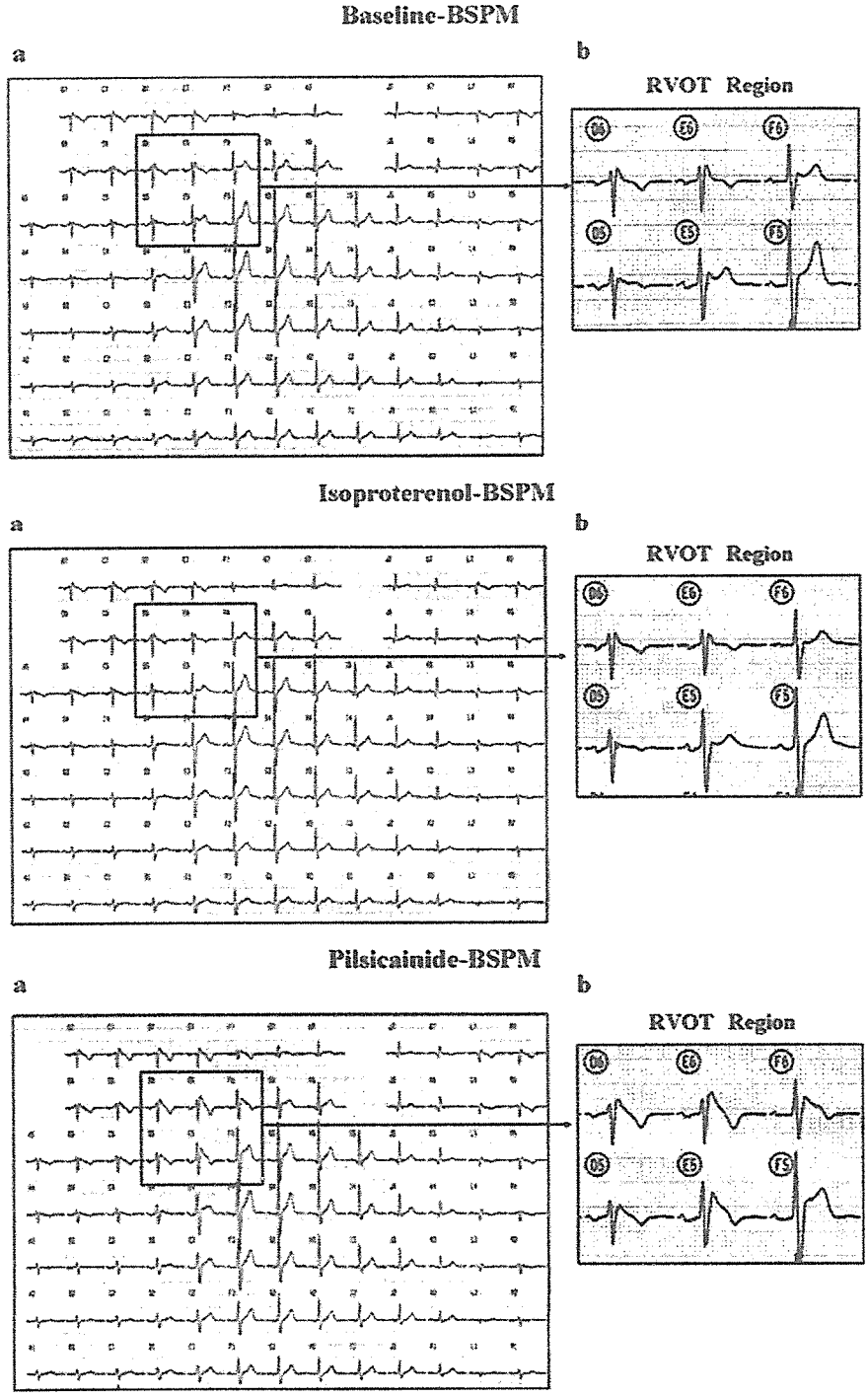

Figure 4. *Eighty-seven-leads electrocardiogram (ECG) (a), and 6-leads ECG (D-F, 5-6) reflecting potentials of the right ventricular outflow tract (RVOT) (b) in a representative patient with Brugada syndrome. (A) Baseline condition. The coved- or saddleback-type ST-segment elevation was seen only in 6-leads, and the mean ST20 was higher in 6-leads (0.17 ± 0.06 mV) than in 81-leads (0.00 ± 0.03 mV). The mean corrected recovery time (RTc) was slightly longer in 6-leads (320 ± 57 ms) than in 81-leads (309 ± 38 ms). The mean QRS duration was slightly prolonged both in 6-leads (109 ± 5 ms) and in 81-leads (102 ± 7 ms), but no major difference was observed between the two regions. (B) Isoproterenol infusion. The ST-segment elevation was normalized in 6-leads (0.07 ± 0.02 mV), but not changed in 81-leads (0.00 ± 0.01 mV). The mean RTc was slightly prolonged with isoproterenol both in 6-leads (346 ± 42 ms) and 81-leads (332 ± 68 ms). The mean QRS duration was not changed with isoproterenol in either 6-leads (102 ± 5 ms) or 81-leads (100 ± 5 ms). (C) Pilsicainide injection. The ST-segment elevation was dramatically augmented only in 6-leads (0.31 ± 0.11 mV), but not changed in 81-leads (0.01 ± 0.04 mV). Pilsicainide prolonged the mean RTc in only 6-leads (336 ± 53 ms), but not in 81-leads (293 ± 42 ms). On the other hand, the mean QRS duration was increased by pilsicainide homogeneously in 6-leads (121 ± 4 ms) and in 81-leads (116 ± 5 ms).*

ECG Parameters Between Patients with *SCN5A* Mutation and Those without *SCN5A* Mutation

The ECG parameters and their changes were compared between 4 patients with *SCN5A* mutation and 24 patients without *SCN5A* mutation. Although the baseline QRS duration was not different between the two groups, the QRS duration after pilsicainide was significantly longer in the *SCN5A* positive patients than in the *SCN5A* negative patients both in 6-leads (138 ± 22 ms vs 123 ± 17 ms; $P < 0.005$) and in 81-leads (134 ± 20 ms vs 119 ± 17 ms; $P < 0.005$).

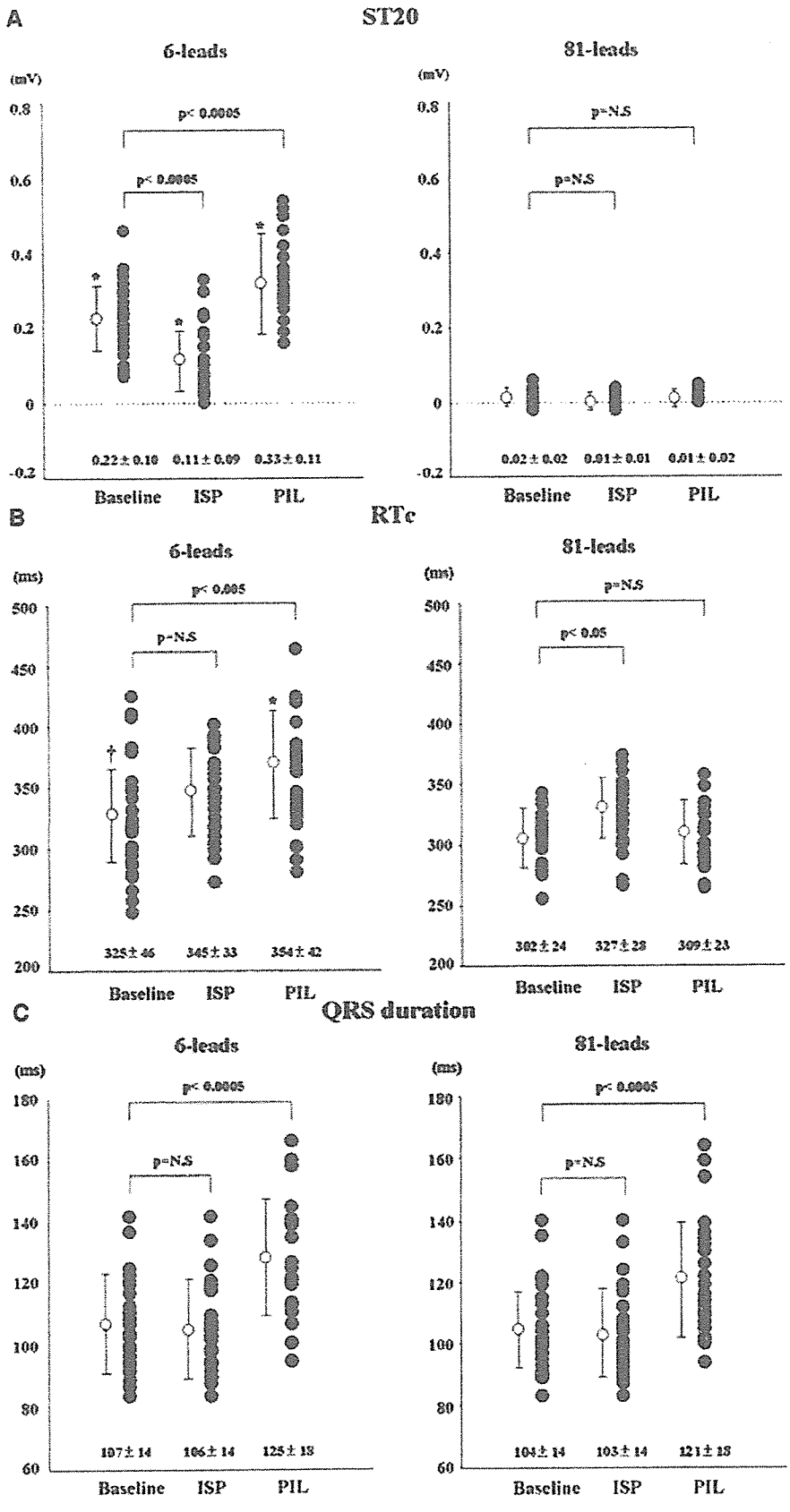

Figure 5. *Composite data of ECG parameters of 6-leads (RVOT region) and 81-leads (Other region) under baseline condition, during isoproterenol infusion (ISP), and after pilsicainide injection (PIL) in the 28 patients with Brugada syndrome. (A) The baseline ST20 was significantly higher in 6-leads than in 81-leads. The ST20 was decreased by isoproterenol and augmented by pilsicainide significantly in 6-leads, while it was not changed in 81-leads. (B) The baseline corrected recovery time (RTc) was longer in 6-leads than in 81-leads. The RTc was significantly prolonged by pilsicainide in only 6-leads. Isoproterenol infusion slightly but significantly prolonged the RTc in 81-leads. (C) The baseline QRS duration was slightly prolonged both in 6-leads and 81-leads. The QRS duration was not changed by isoproterenol, but further increased homogeneously by pilsicainide in both regions. *P < 0.0005, †P < 0.05 versus 81-leads.*

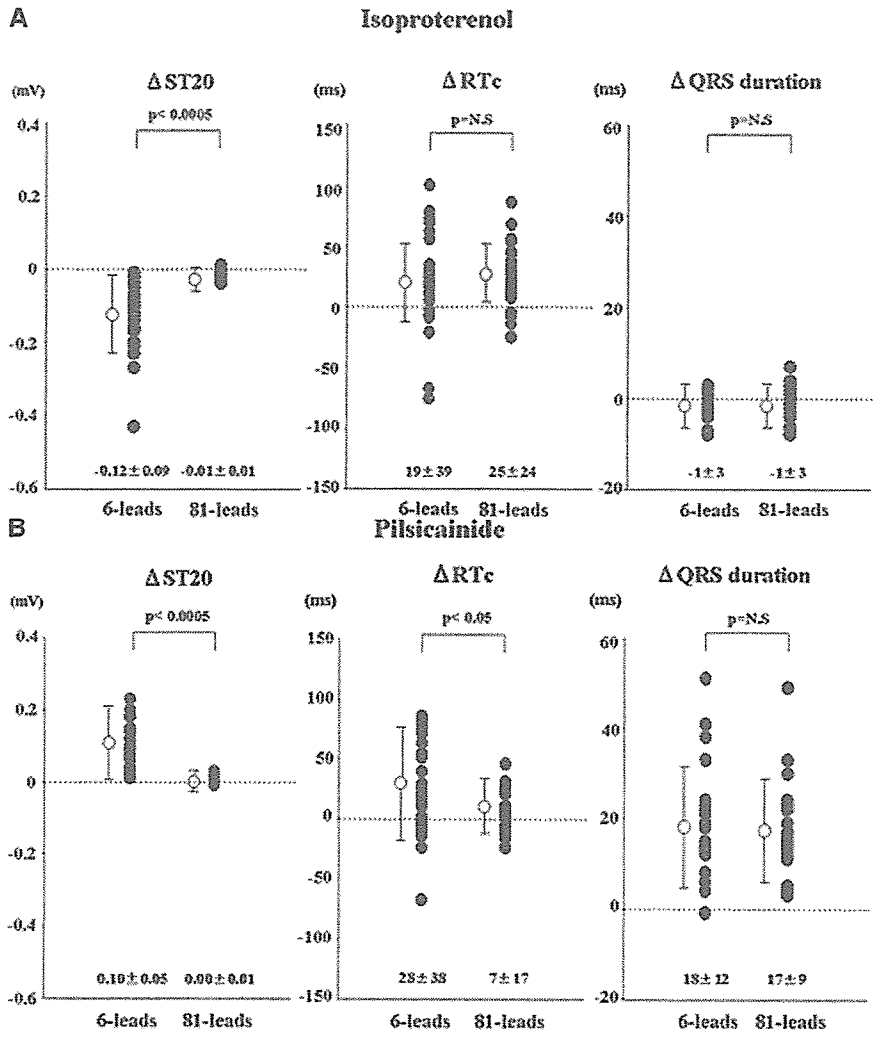

Figure 6. *Comparison of changes (Δ) of ECG parameters with pharmacological interventions between 6-leads (RVOT region) and 81-leads (Other region) in the 28 patients with Brugada syndrome. (A) Isoproterenol infusion. The ΔST20 was significantly larger in 6-leads than in 81-leads, while both ΔRTc and ΔQRS duration were not different between the two regions. (B) Pilsicainide injection. The ΔST20 and the ΔRTc were significantly larger in 6-leads than in 81-leads, while the ΔQRS duration was not different between the two regions.*

The ΔQRS duration with pilsicainide was also significantly larger in the *SCN5A* positive patients than in the *SCN5A* negative patients both in 6-leads (36 ± 16 ms vs 15 ± 8 ms; $P < 0.005$) and in 81-leads (31 ± 15 ms vs 15 ± 6 ms; $P < 0.005$). No significant differences were observed in other ECG parameters and their changes between 4 patients with *SCN5A* mutation and 24 patients without *SCN5A* mutation.

ECG Parameters Between Patients with Spontaneous Type 1 ECG and Those with Sodium Channel Blocker-Induced Type 1 ECG

Since it is generally accepted that Brugada patients with spontaneous Type 1 ECG are at higher risk of cardiac events than those with sodium channel blocker-induced Type 1 ECG, we compared the ECG parameters and the change of the ECG parameters between 17 patients with spontaneous Type 1 ECG and 11 patients with sodium channel blocker-induced Type 1 ECG. There were no significant differences in the ECG parameters between the two groups, except for the ST20 under baseline condition and after isoproterenol and pilsicainide. The changes of each ECG parameter by pharmacological interventions showed similar tendency between the two groups (data not shown).

Discussion

The major findings of the present study were: (1) the ST-segment elevation and RTc prolongation were localized and modulated by pharmacological interventions only in the region of RVOT, and (2) the slight prolongation of QRS duration at baseline and its further increase by a sodium channel blocker, pilsicainide, were observed homogeneously throughout the ventricular wall.

Transmural Electrical Heterogeneity of Repolarization Localized in the RVOT

The ST-segment elevation in the right precordial leads in patients with Brugada syndrome

is thought to result from transmural heterogeneity in action potential (AP) configuration in the RVOT.[15,16] Experimental data using arterially perfused right ventricular wedge preparations have suggested that prominent transient outward current (I_{to})-mediated AP notch and a loss of AP dome in epicardium, but not in endocardium, give rise to a transmural voltage gradient, resulting in ST-segment elevation.[15] Since the maintenance of the epicardial AP dome is determined by the balance of currents active at the end of phase 1 of the AP (principally I_{to} and L-type calcium current (I_{Ca-L})), any interventions that increase outward currents (e.g., I_{to}, slow and fast activating components of delayed rectifier potassium current (I_{Ks}, I_{Kr})) or decrease inward currents (e.g., I_{Ca-L}, fast I_{Na}) can accentuate ST-segment elevation.[16] Among these interventions, class IC sodium channel blockers, such as pilsicainide, most effectively amplify or unmask ST-segment elevation secondary to their strong effect to block fast I_{Na}.[24–26] On the other hand, isoproterenol, a β-adrenergic stimulant, strongly augments I_{Ca-L}, and therefore, attenuates ST-segment elevation.[27]

Several previous studies have examined the spatial distribution of depolarization and repolarization abnormalities by using BSPM system.[28–31] In the present study, we evaluated the ST-segment amplitude (ST20) and the RTc as repolarization parameters. Because the maximum dV/dt point of T wave in the ECG is shown to correspond to the minimum dV/dt point of the epicardial AP, the RT is approximately the sum of the activation time and the AP duration at 90% repolarization in the epicardial cell.[32]

The effect of isoproterenol to normalize the ST-segment elevation in the RVOT region is thought to be as a result of decreased transmural voltage gradient due to decreased phase 1 notch in the epicardial AP. On the other hand, pilsicainide induced the coved-type ST-segment elevation, the terminal negative T wave, and the prolongation of RT only in the RVOT region. These changes in the electrocardiographic phenotype are probably due to the accentuated phase 1 notch and a greater prolongation of the epicardial AP duration or phase 2 reentry-induced second epicardial AP, resulting in reversed transmural voltage gradient between the epicardial and the endocardial APs.

Sodium Channel Defect and Depolarization Abnormality

The first mutation linked to Brugada syndrome was identified in *SCN5A*, the gene encoding α-subunit of the sodium channel; and functional studies of *SCN5A* mutations responsible for the Brugada phenotype have demonstrated the "loss of function" of I_{Na} by several mechanisms.[17]

Mild conduction abnormalities, such as widening of P wave, prolongation of QRS duration, PQ interval and HV interval, and higher incidence of right bundle-branch block, have been described in patients with Brugada syndrome.[8,12] Signal-averaged ECG recordings have demonstrated late potentials in approximately two-thirds of Brugada patients.[5] Some *SCN5A* mutations responsible for Brugada phenotype are reported to be associated with more severe conduction disease (i.e., depolarization abnormalities). Moreover, recent histological studies in patients with Brugada syndrome have shown the presence of concealed structural abnormalities and conduction slowing in the RVOT area.[33,34]

We recently conducted a high-resolution optical mapping in an experimental Brugada model employing a canine right ventricular wedge preparation, which allowed a detailed measurement of cellular repolarization and depolarization in the epicardial and endocardial surfaces.[35] Our data suggested that the initiating ventricular premature beats were caused by phase 2 reentry originated from the epicardial area with a steep gradient of ventricular repolarization time due to heterogeneous loss of the AP dome. In contrast, wave-break appeared at sites of delayed epicardial conduction during the first few reentrant waves, which was closely associated with VF susceptibility, suggesting that conduction abnormalities contribute to the maintenance of VF under the Brugada condition.

It is still unclear whether depolarization abnormalities are localized in the region of RVOT or distributed homogeneously in the whole ventricle. We measured the QRS duration from all 87-leads BSPM as a depolarization parameter by using our original algorithm in the present study. Mild prolongation of the QRS duration under baseline condition and its further prolongation by a sodium channel blocker were observed homogeneously between the RVOT region and the other region. Our data suggest that depolarization abnormality is distributed homogeneously throughout the ventricle, probably due to sodium channel dysfunction.

Study Limitations

First limitation of the present study is that the electrocardiographic measurements were made in the body surface region, but not in the ventricular wall directly. There is no one-to-one correspondence between the measurements from the body surface and those from the ventricular wall. This is because every electrode on the body surface records potentials that are generated by activity in the entire heart, although weighted by proximity.

Second, we measured RT but not QT interval as a repolarization parameter in the present study,

because the QT interval is difficult to measure semi-automatically. Moreover, the end of the QT interval is expected to coincide with full repolarization of several cell types, depending on the morphology of the T wave. In the case of saddleback-type ST elevation and coved-type ST elevation without negative T wave, repolarization of the epicardial AP is earlier than that of the endocardial AP, and thus repolarization of subendocardial cell coincides with the end of the QT interval. On the other hand, in the case of coved-type ST elevation with negative T wave, repolarization of the epicardial AP is later than that of the endocardial AP, and thus repolarization of epicardial cell coincides with the end of the QT interval. As a depolarization parameter, we examined the QRS duration, but not the ventricular activation time (VAT) defined as the interval between QRS-onset and minimum dV/dt point of the QRS. This was because the accentuated J-point and ST-segment elevation are superimposed on the late r' wave in the right precordial leads in patients with Brugada syndrome; thus the VAT seems to be overestimated in the RVOT region.

Acknowledgments: Dr. W. Shimizu was supported by the Hoansha Research Foundation; Japan Research Foundation for Clinical Pharmacology; Ministry of Education, Culture, Sports, Science and Technology Leading Project for Biosimulation; and health sciences research grants (H18—Research on Human Genome, Tissue Engineering) from the Ministry of Health, Labour and Welfare, Japan.

References

1. Brugada P, Brugada J. Right bundle branch block, persistent ST segment elevation and sudden cardiac death: A distinct clinical and electrocardiographic syndrome: A multicenter report. J Am Coll Cardiol 1992; 20:1391–1396.
2. Brugada J, Brugada P. Further characterization of the syndrome of right bundle branch block, ST segment elevation, and sudden cardiac death. J Cardiovasc Electrophysiol 1997; 8:325–331.
3. Brugada J, Brugada R, Brugada P. Right bundle-branch block and ST-segment elevation in V1 through V3. A marker for sudden death in patients without demonstrable structural heart disease. Circulation 1998; 97:457–460.
4. Wilde AA, Antzelevitch C, Borggrefe M, et al. Study group on the molecular basis of arrhythmias of the European society of cardiology. Proposed diagnostic criteria for the Brugada syndrome: Consensus report. Circulation 2002; 106:2514–2519.
5. Antzelevitch C, Brugada P, Borggrefe M, et al. Brugada syndrome: Report of the second consensus conference: Endorsed by the Heart Rhythm Society and the European Heart Rhythm Association. Circulation 2005; 111:659–670.
6. Antzelevitch C, Brugada P, Borggrefe M, et al. Brugada syndrome: Report of the second consensus conference. Heart Rhythm 2005; 2:429–440.
7. Priori SG, Napolitano C, Gasparini M, et al. Natural history of Brugada syndrome: Insights for risk stratification and management. Circulation 2002; 105:1342–1347.
8. Priori SG, Napolitano C, Memmi M, et al. Clinical and genetic heterogeneity of right bundle branch block and ST-segment elevation syndrome: A prospective evaluation of 52 families. Circulation 2000; 102:2509–2515.
9. Shimizu W, Aiba T, Kamakura S. Mechanisms of diseases: Current understanding and future challenges in Brugada syndrome. Nat Clin Pract Cardiovasc Med 2005; 2:408–414.
10. Nademanee K, Veerakul G, Nimmannit S, et al. Arrhythmogenic marker for the sudden unexplained death syndrome in Thai men. Circulation 1997; 96:2595–2600.
11. Pitzalis MV, Anaclerio M, Iacoviello M, et al. QT-interval prolongation in right precordial leads: An additional electrocardiographic hallmark of Brugada syndrome. J Am Coll Cardiol 2003; 42:1632–1637.
12. Smits JP, Eckardt L, Probst V, et al. Genotype-phenotype relationship in Brugada syndrome: Electrocardiographic features differentiate SCN5A-related patients from non-SCN5A-related patients. J Am Coll Cardiol 2002; 40:350–356.
13. Nagase S, Kusano KF, Morita H, et al. Epicardial electrogram at the right ventricular outflow tract in patients with the Brugada syndrome: Using the epicardial leads. J Am Coll Cardiol 2002; 39:1992–1995.
14. Antzelevitch C. Late potentials and the Brugada syndrome. J Am Coll Cardiol 2002; 39:1996–1999.
15. Yan GX, Antzelevitch C. Cellular basis for the Brugada syndrome and other mechanisms of arrhythmogenesis associated with ST-segment elevation. Circulation 1999; 100:1660–1666.
16. Antzelevitch C. The Brugada syndrome: Ionic basis and arrhythmia mechanisms. J Cardiovasc Electrophysiol 2001; 12:268–272.
17. Meregalli PG, Wilde AA, Tan HL. Pathophysiological mechanisms of Brugada syndrome: Depolarization disorder, repolarization disorder, or more? Cardiovasc Res 2005; 67:367–378.
18. Roden DM, Wilde AA. Drug-induced J point elevation: A marker for genetic risk of sudden death or ECG curiosity? J Cardiovasc Electrophysiol 1999; 10:219–223.
19. Shimizu W, Kamakura S, Kurita T, Suyama K, Aihara N, Shimomura K. Influence of epinephrine, propranolol, and atrial pacing on spatial distribution of recovery time measured by body surface mapping in congenital long QT syndrome. J Cardiovasc Electrophysiol 1997; 8:1102–1114.
20. Shimizu W, Matsuo K, Takagi M, et al. Body surface distribution and response to drugs of ST segment elevation in Brugada syndrome: Clinical implication of eighty-seven-lead body surface potential mapping and its application to twelve-lead electrocardiograms. J Cardiovasc Electrophysiol 2000; 11:396–404.
21. Kamakura S, Shimizu W, Matsuo K, et al. Localization of the optimal ablation site of idiopathic ventricular tachycardia from right and left ventricular outflow tract by body surface electrocardiogram. Circulation 1998; 98:1525–1533.
22. Tahara N, Takaki H, Taguchi A, et al. Exercise-induced QRS prolongation in patients with mild coronary artery disease: Computer analysis of the digitized multilead ECGs. J Electrocardiol 1999; 32:206–211.
23. Sakuragi S, Takaki H, Taguchi A, et al. Diagnostic value of the recovery time-course of ST slope on exercise in discriminating false-from true-positive ST-segment depressions. Circ J 2004; 68:915–922.
24. Krishnan SC, Josephson ME. ST segment elevation induced by class IC antiarrhythmic agents: Underlying electrophysiologic mechanisms and insights into drug-induced proarrhythmia. J Cardiovasc Electrophysiol 1998; 9:1167–1172.
25. Fujiki A, Usui M, Nagasawa H, Mizumaki K, Hayashi H, Inoue H. ST segment elevation in the right precordial leads induced with class IC antiarrhythmic drug: Insight into the mechanism of Brugada syndrome. J Cardiovasc Electrophysiol 1999; 10:214–218.
26. Shimizu W, Antzelevitch C, Suyama K, et al. Effect of sodium channel blockers on ST segment, QRS duration, and corrected QT interval in patients with Brugada syndrome. J Cardiovasc Electrophysiol 2000; 11:1320–1329.
27. Miyazaki T, Mitamura H, Miyoshi S, Soejima K, Aizawa Y, Ogawa S. Autonomic and antiarrhythmic drug modulation of ST segment elevation in patients with Brugada syndrome. J Am Coll Cardiol 1996; 27:1061–1070.
28. Eckardt L, Bruns HJ, Paul M, et al. Body surface area of ST elevation and the presence of late potentials correlate to the inducibility of ventricular tachyarrhythmias in Brugada syndrome. J Cardiovasc Electrophysiol 2002; 13:742–749.
29. Bruns HJ, Eckardt L, Vahlhaus C, et al. Body surface potential mapping in patients with Brugada syndrome: Right precordial ST segment variations and reverse changes in left precordial leads. Cardiovasc Res 2002; 54:58–66.
30. Hisamatsu K, Kusano KF, Morita H, et al. Relationships between depolarization abnormality and repolarization and abnormality